2

CR 114507
Available to Public

GULF GENERAL ATOMIC

GULF-GA-A12242

STUDY OF RADIOISOTOPE SAFETY DEVICES FOR ELECTRIC PROPULSION SYSTEM

VOLUME III - BRIEFING AND REVIEW OF WORK

By

G. B. Bradshaw, W. G. Homeyer, F. D. Postula, and E. J. Steeger

Prepared under Contract No. NAS 2-5891 by
GULF GENERAL ATOMIC COMPANY
San Diego, California

for

AMES RESEARCH CENTER

NATIONAL AERONAUTICS AND SPACE ADMINISTRATION

September 1972

GULF GENERAL ATOMIC COMPANY
P.O. BOX 608, SAN DIEGO, CALIFORNIA 92112

GULF GENERAL ATOMIC

GULF-GA-A12242

STUDY OF RADIOISOTOPE SAFETY DEVICES FOR ELECTRIC PROPULSION SYSTEM

VOLUME III - BRIEFING AND REVIEW OF WORK

By

G. B. Bradshaw, W. G. Homeyer, F. D. Postula, and E. J. Steeger

Prepared under Contract No. NAS 2-5891 by

GULF GENERAL ATOMIC COMPANY

San Diego, California

for

AMES RESEARCH CENTER
NATIONAL AERONAUTICS AND SPACE ADMINISTRATION

Gulf General Atomic Project 2113 September 1972

GULF GENERAL ATOMIC COMPANY
P.O. BOX 608, SAN DIEGO, CALIFORNIA 92112

FORWARD

This slide brochure is the third volume of a final report on the second phase of a study on radioisotope--thermionic power supply for electric propulsion to the outer planets. The first phase focused on the design and operational details for the 5 kW(e) thermonic power supply, which is fueled with 44.2 kW(t) of $^{244}Cm_2O_3$. Phase-II concentrated on the design and analysis of safety equipment to protect against dispersal of the isotope fuel. The safety equipment in this design is a passive containment system which does not rely on the operation of any mechanism, such as a launch escape rocket or deployment of parachutes.

Volume I of this report is a summary report and Volume II is the complete technical report.

The major mission and system constraints on which the study was based are given in the table. The full power level of 5 kWe is required during the first 10,000 hours and the last 10,000 hours of the mission, with low power required during the intervening 6,000 hours. Safety equipment required to prevent the isotope from being dispersed as a result of a launch accident is jettisoned after the power supply attains hyperbolic speed relative to the earth.

MISSION AND SYSTEM CONSTRAINTS

RADIOISOTOPE	CM-244
POWER LEVEL	5 KW(E)
MISSION DURATION	36,000 HRS
LAUNCH VEHICLE	TITAN III-D/CENTAUR
LAUNCH TRAJECTORY	DIRECT INJECTION TO HYPERBOLIC
SAFETY PHILOSOPHY	INTACT THROUGH IMPACT
SAFETY EQUIPMENT	JETTISONED AFTER LAUNCH

At launch, the reference design power supply consists of the radioisotope heat source, the converter assembly, and safety equipment. The heat source consists of the radioisotope capsules and the capsule holder. The converter assembly includes emitter heat pipes, thermionic converters, electrical leads, a beryllium neutron shield, and a space radiator. The safety equipment includes an auxiliary cooling system with heat pipes and a water circulation system, lithium hydride neutron shielding, a secondary containment vessel for the radioisotope, a reentry shield, a fire shield, an enlarged aerodynamic flare, and an impact energy absorber.

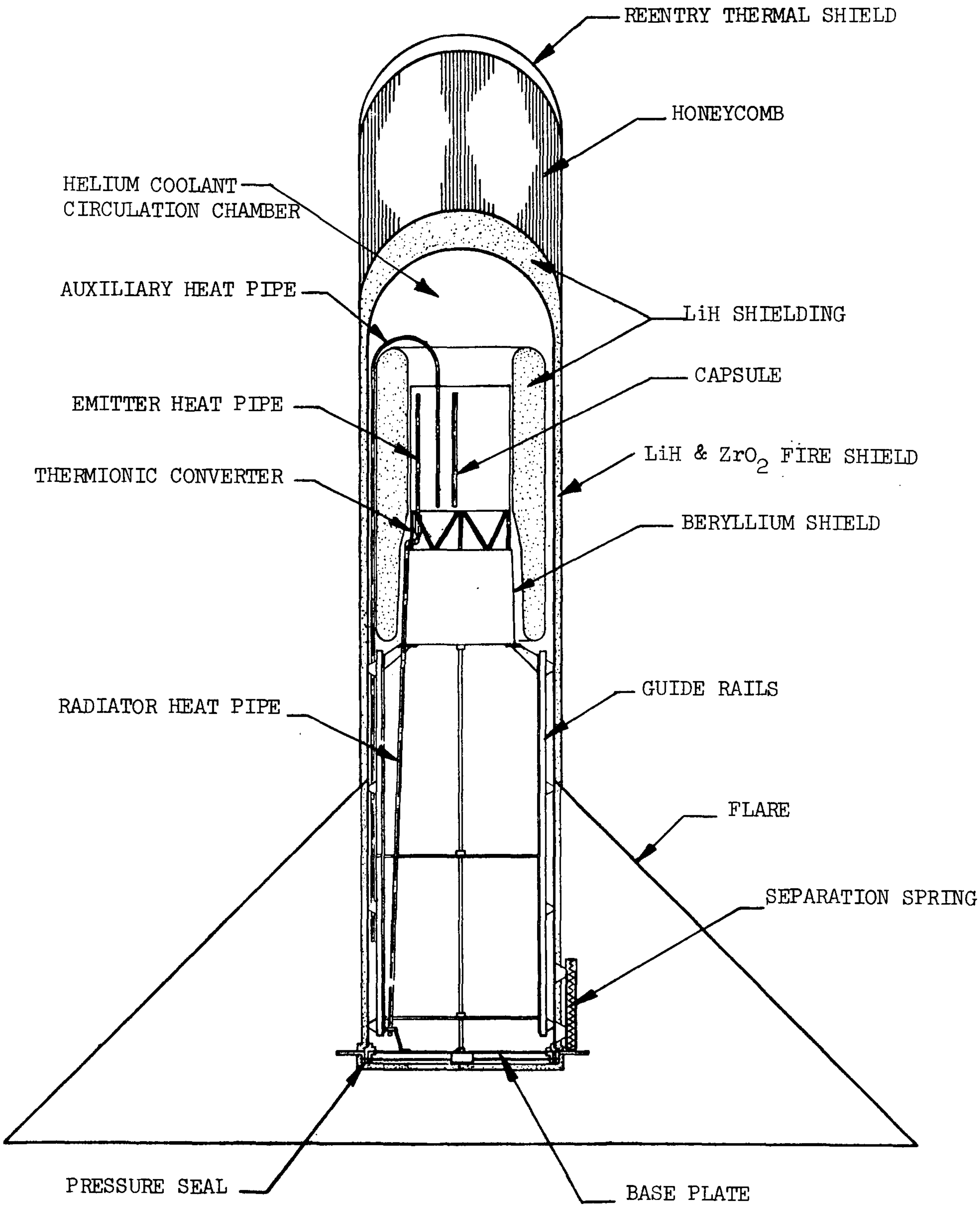

a) OVERALL VIEW

The cylindrical outer shell of the safety equipment is 0.556 meter in diameter by 3.11 meters long. The 2.44 meter base diameter of the aerodynamic flare in the reference design can be increased to as much as 0.6 meters to produce a lower hypersonic ballistic coefficient.

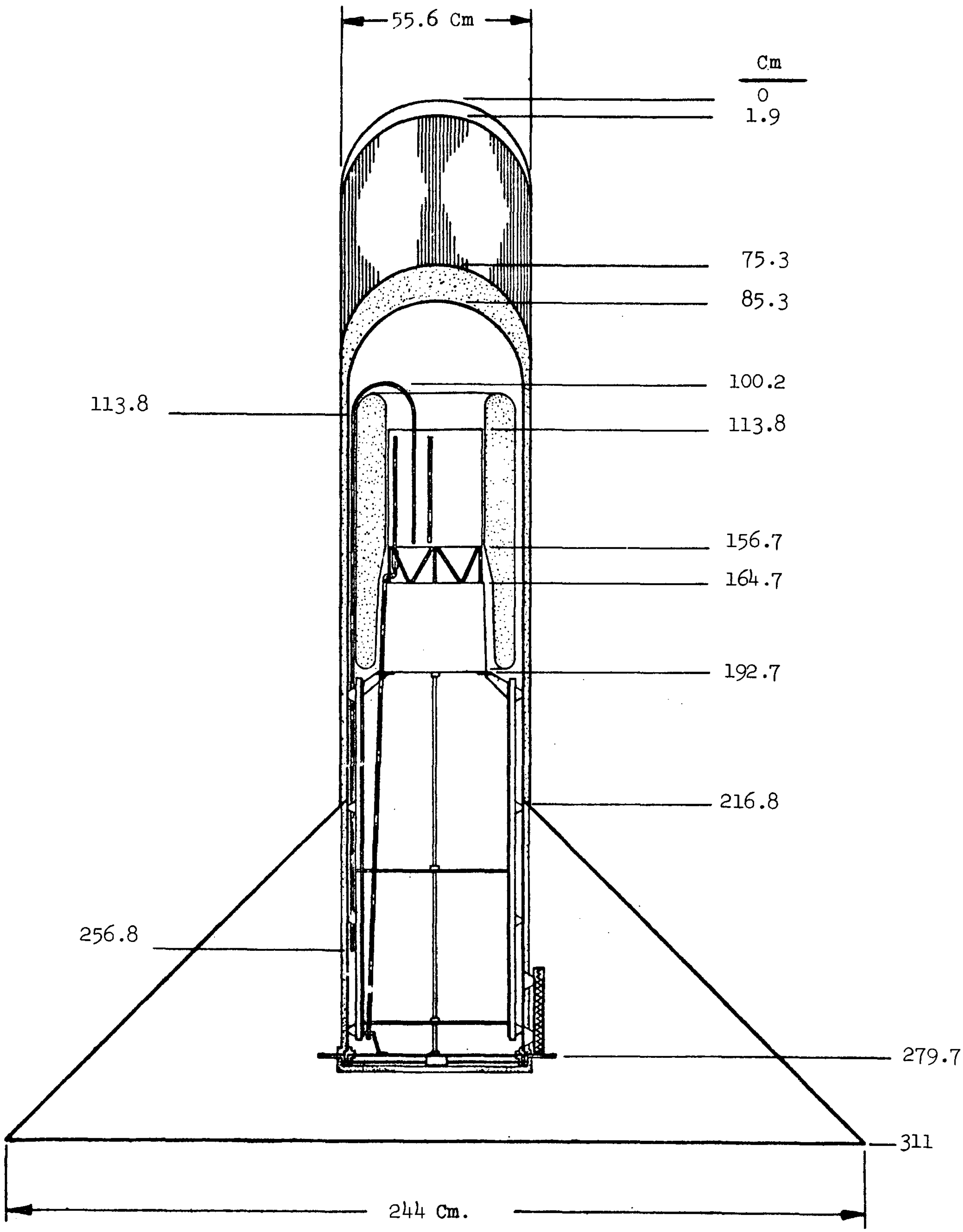
55.6 Cm
Cm
0
1.9
75.3
85.3
100.2
113.8
113.8
156.7
164.7
192.7
216.8
256.8
279.7
311
244 Cm.

After the power supply has been accelerated to hyperbolic speed relative to the earth, the secondary containment is opened by breaking the seal between the flight system and safety equipment. The flight system is withdrawn from the safety equipment, removing the auxiliary heat pipes from within the radioisotope heat source.

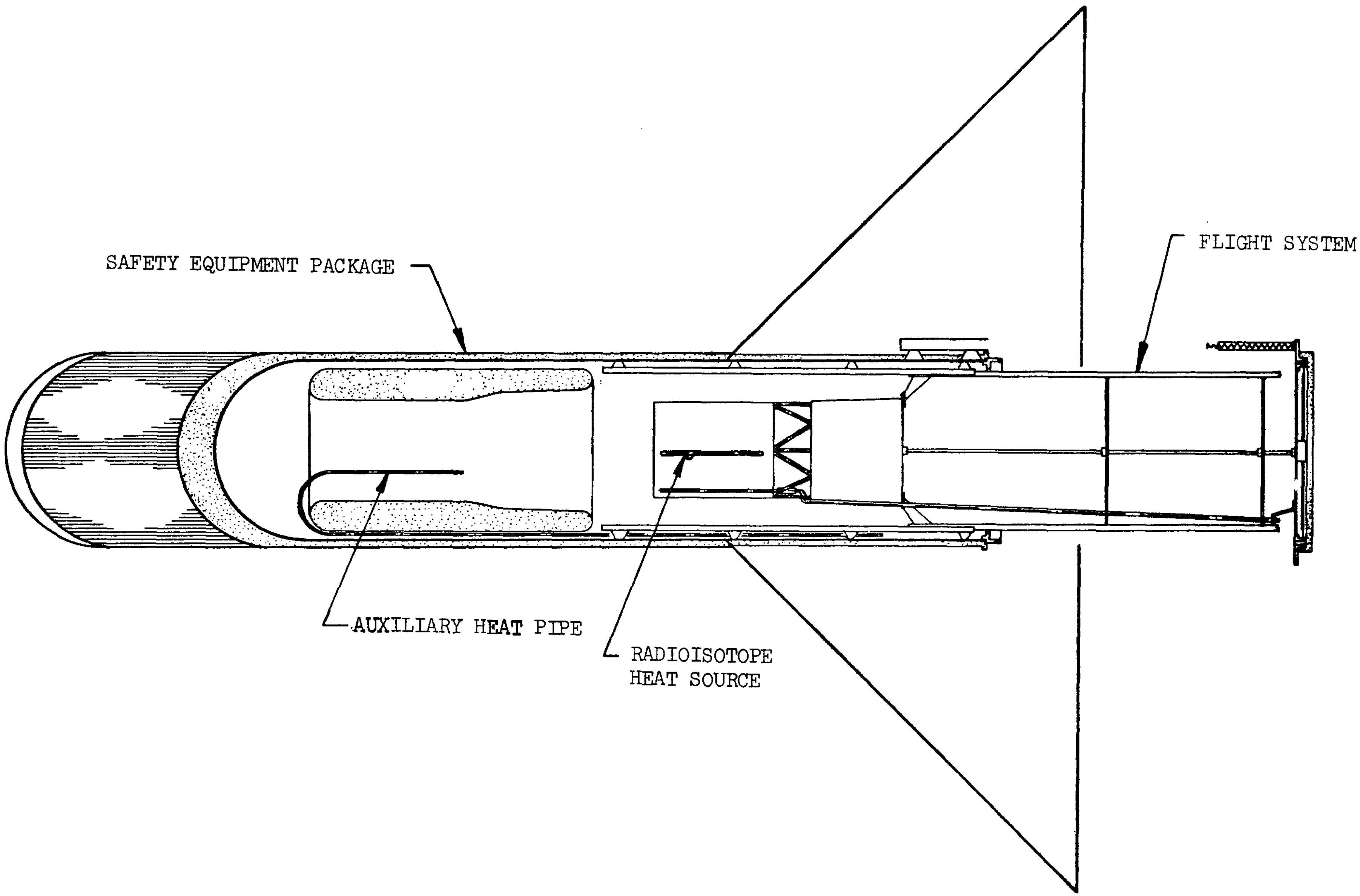

Separation of safety equipment from flight system

The configuration of the radioisotope power supply in heliocentric flight is shown. A portion of the radioisotope heat generated in the heat source is converted to electricity in the thermionic converters and transmitted to the power conditioning equipment which is located at the payload. The waste heat is transferred through the nuclear radiation shield and radiated to space from the radiator heat pipes.

FLIGHT CONFIGURATION

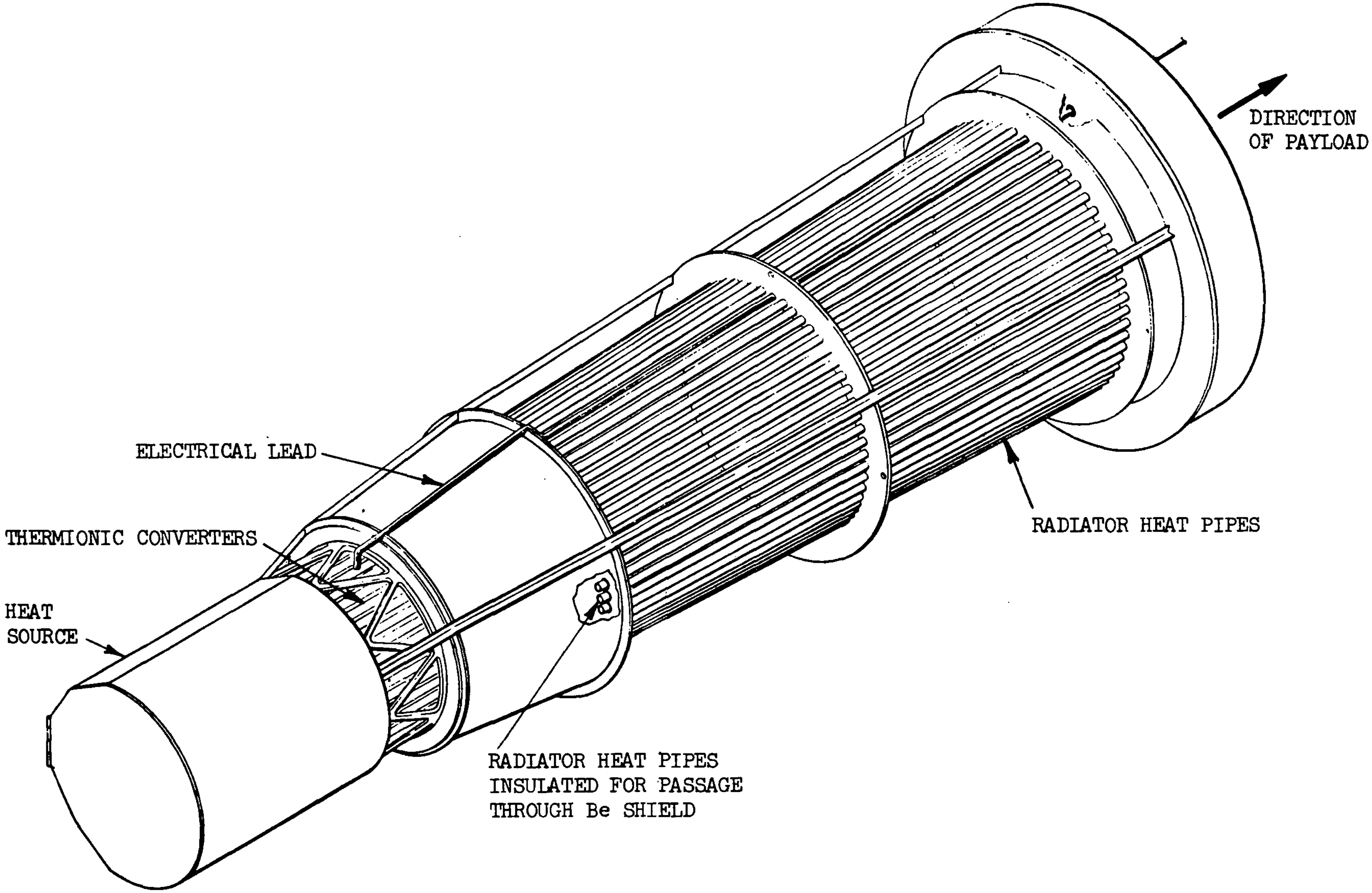

The $^{244}Cm_2O_3$ radioisotope is contained in 136 capsules of tungsten 25% rhenium alloy. Each capsule is sized to allow void volume for helium accumulation over a period of 150 days. During the mission the helium gas is released through a porous plug of tungsten 25% rhenium alloy. The plug is sized to maintain a helium pressure over the fuel to suppress the vaporization of fuel.

ISOTOPE FUEL CAPSULE

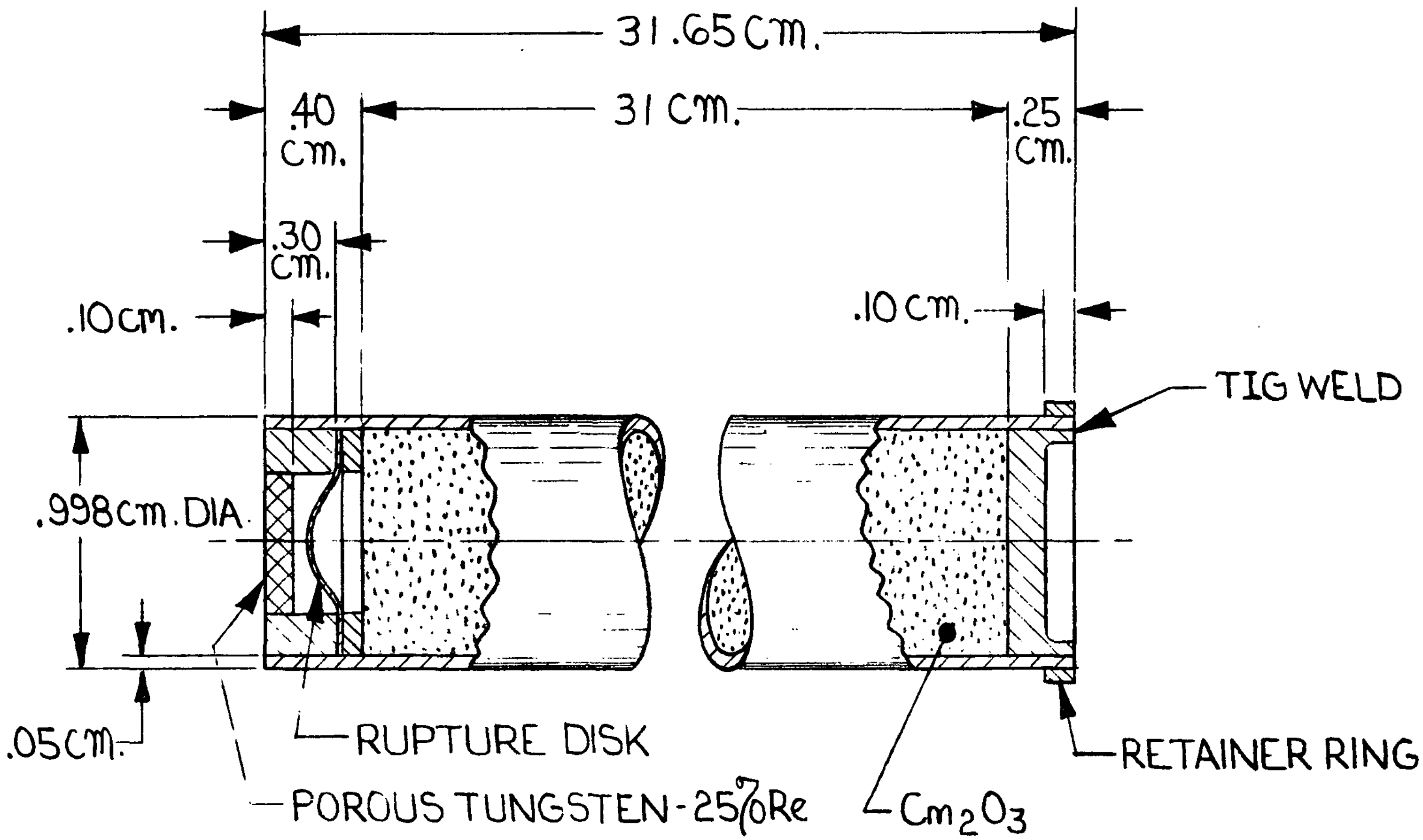

Heat is transferred from the radioisotope capsules to the emitter heat pipes by thermal radiation. In the launch configuration, there are auxiliary heat pipes inserted between the radioisotope capsules and the emitter heat pipes which remove the isotopic heat by conduction through helium gas. The heat source is covered with multi-foil thermal insulation to reduce heat leakage.

RADIOISOTOPE HEAT SOURCE

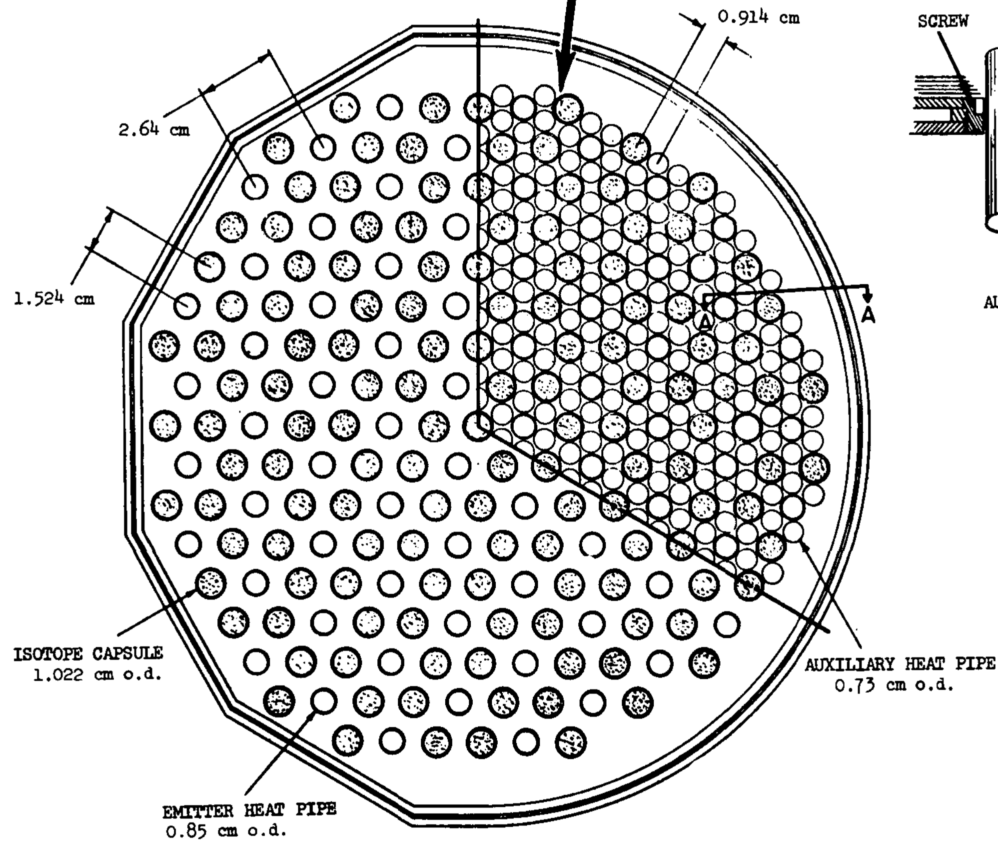

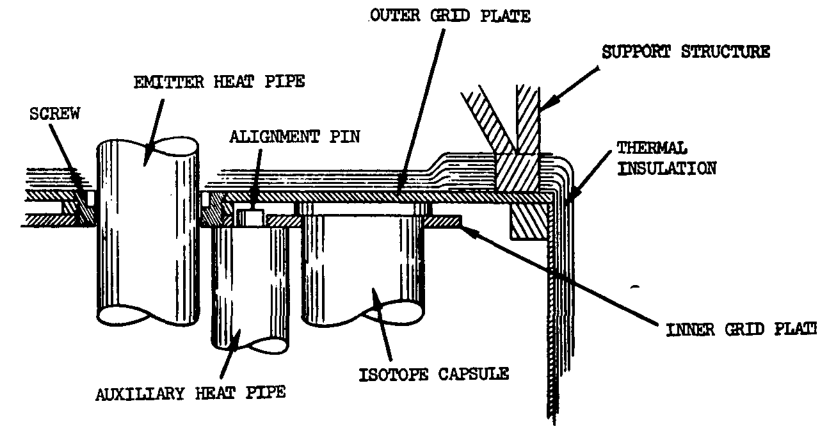

SECTION A-A

The thermionic converter consists of a tungsten emitter and niobium collector with cesium pressure maintained in the interelectrode space by a graphite sorption-type cesium reservoir. Heat is transferred to the emitter by a heat pipe integral with the emitter. The vapor space in the heat pipe is separated from the liquid space by a porous tube. Heat is removed from the collector of the thermionic converter by a collector heat pipe. The radiator heat pipe is inserted in the socket in the base of the collector heat pipe.

THERMIONIC CONVERTER

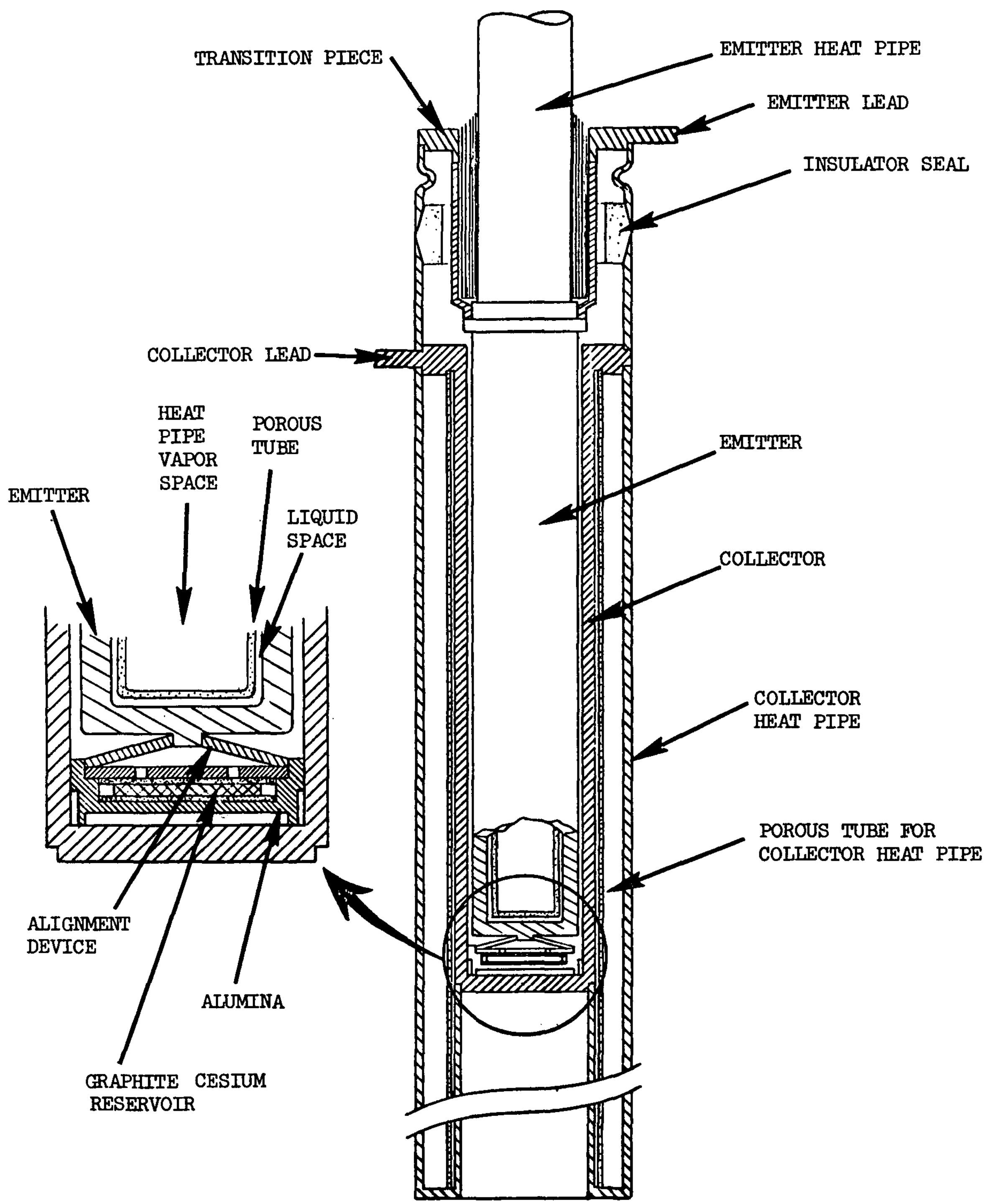

Of the 69 thermionic converter modules in operation at the beginning of life (BOL), it is assumed that 59 will remain in operation at the end of life (EOL). The reduction in net output over the lifetime of the power supply results from decay of the radioisotope fuel as well as the postulated failure of 10 of the converter modules.

ELECTRICAL PERFORMANCE PARAMETERS

	BOL	EOL
NUMBER OF OPERATING CONVERTERS	69	59
NET OUTPUT (KWE)	5.93	5.00
OVERALL EFFICIENCY (%)	13.4	13.2
TOTAL THERMAL POWER (KWT)	44.2	37.78
VOLTAGE TO P. C. (VOLTS)	15.2	14.9

The mass of the power supply prior to jettison of the safety equipment is 723.5 kg which represents the sum of the masses of the flight system and of the safety equipment.

SYSTEM MASS SUMMARY

EXTENDED MISSION SYSTEM	148.5 KG
DISPOSABLE SAFETY EQUIPMENT	575.3 KG
TOTAL MASS AT LAUNCH	723.8 KG

This chart shows the distribution of mass for the major flight system components. The total flight system mass is 155.5 kg, which results in a system flight specific power of 284 watts (el)/kg. A large portion of the mass is attributed to the beryllium neutron shield (25%), which is designed to limit the neutron dose to $< 10^{12}$ not over a two-meter diameter plane in 36,000 hours, and to power conditioning and transmission (30%).

MASS OF FLIGHT SYSTEM COMPONENTS

CURIUM ISOTOPE CAPSULES	29.2 kg
HEAT SOURCE STRUCTURE, INSULATION	15.5 kg
EMITTER HEAT PIPES, TI DIODES	15.4 kg
RADIATOR HEAT PIPES, RADIATOR	9.5 kg
BERYLLIUM NEUTRON SHIELD, BLAST SHIELD	30.0 kg
TRANSMISSION LINES, BOOMS, POWER CONDITIONER	48.9 kg
TOTAL	148.5 kg

This table gives a breakdown of the major safety system components and their design masses. This system represents 79% of the launch mass, but has only a small influence on payload mass since it is ejected early in the mission. Most of the safety system mass is associated with reentry protection (26%), structure (25%) and the fire shield (12%).

MASS OF DISPOSABLE SAFETY SYSTEM COMPONENTS

REENTRY HEATING PROTECTION	152.0 kg
IMPACT PROTECTION MASS	60.8 kg
ZIRCONIA/LiH FIRE SHIELD	67.5 kg
LiH BIOLOGICAL SHIELD	78.6 kg
STRUCTURE, LAUNCH COOLING, JETTISON EQ.	143.5 kg
AUXILIARY RADIATOR	32.5 kg
BLAST SHIELD, RECOVERY AIDS	40.4 kg
TOTAL	575.3 kg

A summary of the electrical power output from the system at beginning-of-life (BOL) and end-of-life (EOL), after 36,000 hours, is shown. Also shown is summary of the masses of the major components of the system and overall dimensions. From this chart it is seen that the total mass at launch is 730.8 kg while the mass of the extended mission flight system is 155.5 kg.

RADIOISOTOPE THERMIONIC POWER SUPPLY DESIGN AND PERFORMANCE SUMMARY

ELECTRICAL	BOL	EOL
NUMBER OF OPERATING CONVERTERS	69	59
NET OUTPUT (kWe)	5.93	5.0
OVERALL EFFICIENCY (%)	13.4	13.2
TOTAL THERMAL POWER (kWt)	44.2	37.77
VOLTAGE TO P.C. (VOLTS)	15.2	14.9

PHYSICAL	
FLIGHT SYSTEMS MASS	148.5 KG
SAFETY SYSTEM MASS	575.3 KG
TOTAL MASS	723.8 KG
OVERALL LENGTH	3.11 METERS
SAFETY RADIATOR DIAMETER	0.556 METERS
FLARE DIAMETER	2.44 METERS

The two primary functions of the safety equipment are to prevent dispersion of Cm-244 in the event of launch accidents, and to protect against radiation. The safety equipment is designed to maintain double containment of the radioisotope through such potential accidents as launch pad fires and explosions, reentry into the atmosphere, and impact on land. Radiation protection includes launch personnel and persons in the vicinity of a power supply which has impacted on land.

SAFETY CRITERIA

- PREVENT DISPERSION OF CM-244
- MAINTAIN DOUBLE CONTAINMENT
    - LAUNCH PAD FIRES AND EXPLOSIONS
    - REENTRY INTO ATMOSPHERE
    - IMPACT ON LAND
- PROTECT AGAINST RADIATION
    - LAUNCH PERSONNEL
    - AFTER IMPACT ON LAND

The major safety design criteria considered in this study were:

1. Containment during a launch pad abort of a Titan IIID/Centaur vehicle, including survival during a 10-minute 2600°K solid propellant fire environment

2. Safety System protection during an ascent abort and resulting explosion shrapnel

3. Fuel and Safety System protection for worst-case atmospheric reentry trajectories

4. Fuel structural and thermal protection during terminal velocity impact onto land

5. Radiation shielding to minimize exposure of operating personnel and persons in the vicinity of an aborted system.

All of these design criteria were met using passive and redundant components, which are listed on the adjacent chart.

RTPS SAFETY PACKAGE SUBSYSTEMS

1. Passive orientated reentry aeroshell with spherical nose and aerodynamic flare
2. Pyro-Carb ablator with zirconia felt insulation backing for reentry protection
3. Auxiliary heat pipe radiator
4. Auxiliary radiator solid propellant fire protection shield
5. Honeycomb terminal velocity impact energy absorber
6. Launch pad helium circulation cooling chamber
7. Blast shield for fragment protection
8. Location aids for land and water impact

A launch pad abort thermal model for the Titan IIID/Centaur was prepared based on existing models for RTG systems. Temperatures and fire durations for the different propellants based on these models are shown in this table. The most severe potential environment occurs when the RTPS lands next to a large chunk of burning solid propellant. In this case, the fire temperature could be as high as 2600°K and last for 600 seconds. To be conservative in the fire shield design, this worst-case condition was assumed.

RADIANT HEAT INPUT TO SAFETY SYSTEM FROM LAUNCH PAD FIRE

SOURCE	TEMPERATURE	DURATION	HEAT INPUT TO SYSTEM	HEAT INPUT/ HEAT GENERATION
Liquid Propellants	5000°F-4000°F (3000-2500°K)	4.8 seconds	$2.3(10)^7$ joules	92
Solid Propellants (1)	4250°F (2616°K)	10 minutes	$2.3(10)^9$ joules	74
Solid Propellant (2)	3000°F (1922°K)	30 minutes	$2.0(10)^9$ joules	21
After Fire (Liquid Propellants)	1850°F (1283°K)	30 minutes	$4.0(10)^8$ joules	4.3

(1) Titan IIIC fire model presented by GE

(2) Solid fire temperature used by AVCO for Isotope Brayton

Extensive design analysis, using detailed two dimensional transient thermal analyzer computer codes, were performed on alternative fire protection concepts listed on the following chart. Most of these were ruled unsatisfactory due to excessive mass or inability to reject the isotope heat from the auxiliary radiator due to excessive temperature drops across the shield. Although some would be satisfactory if they could be removed immediately after a launch fire, this was considered an undesirable system constraint.

LAUNCH PAD FIRE PROTECTION
CONCEPTS INVESTIGATED

- HEAT STORAGE
- INSULATION
- INSULATION/HEAT STORAGE
- THERMAL SWITCH MATERIALS
- DIFFERENTIAL EXPANSION RADIATION SHIELDS
- MODIFIED AUXILIARY RADIATOR DESIGN

The capability of the RTPS to survive probable reentry abort environment was determined by analysing the aerodynamic heating and ablation for various reentry trajectories. Primary reentry protection is provided by a layer of graphite over all exposed surfaces. This is backed up by zirconia felt insulation to reduce the temperature rise of the containment structure.

REENTRY HEAT SHIELD DESIGN

ALTERNATE ABORT CONFIGURATIONS CONSIDERED

- RTPS NOSE FORWARD ATTITUDE SELECTED

RANGE OF REENTRY TRAJECTORIES SUPPLIED BY NASA AMES CONSIDERED

- FLIGHT PATH ANGLES FROM -10^{o} TO -90^{o}
- 90^{o} LAUNCH AZIMUTH
- LOW EARTH ORBIT REENTRY

TRANSIENT AERODYNAMIC HEATING ANALYSIS FOR BRACKETING WORST CASE

THERMAL PROTECTION SYSTEM SELECTED FOR ANALYSIS

- PYROCARB 406 ABLATOR
- ZIRCONIA FELT INSULATION
- STAINLESS STEEL STRUCTURE

TRANSIENT MASS LOSS RATES OF ABLATOR COMPUTED

The safety system design also considered the effects of fragments and shrapnel from a booster explosion. Although the RTPS would likely be located on top of the spacecraft during launch, and thus be shielded from most of the blast environment, a thin titanium shield was added to attenuate and fragment large pieces of explosion shrapnel. This shield is used primarily to protect the aerodynamic flare and auxiliary radiator from extensive damage. Shielding of the fuel capsules is provided by the flare and radiator structure, the Be shield and the heat source structure.

BLAST SHIELD DESIGN

PURPOSE:	PROTECT SAFETY SUBSYSTEMS FROM BOOSTER EXPLOSION FRAGMENTS (TITAN III D/CENTAUR VEHICLE)
DESIGN APPROACH:	EMPIRICAL, BASED ON FLIGHT ISOTOPE HEATER AND RTG DESIGN
DESIGN SELECTED:	TITANIUM SHIELD 0.64 CM. OVER FLIGHT SYSTEM 0.13 CM. OVER FLARE BASE TOTAL MASS: 31.7 KG

Recovery aids are incorporated into the safety package for locating the RTPS following an accidental abort impact onto land or water. These devices are stored in flare envelopes and protected from both the thermal and blast environment. The objective of the recovery aids is to assist search teams in locating the RTPS in the shortest possible time.

POST IMPACT LOCATION AIDS

OCEAN IMPACT:	TRAJECTORY DATA
	RADIO BEACON
	FLASHING LIGHT
	DYE MARKER
	FLOTATION BAGS
	UNDERWATER ACOUSTIC BEACONS
	RADAR CHAFT AND REFLECTIVE COATINGS
LAND IMPACT:	TRAJECTORY DATA
	RADIO BEACON
	THERMAL SIGNATURE OF SOURCE
	RADAR CHAFT AND REFLECTIVE COATINGS
RECOVERY SUPPORT:	AIRCRAFT SEARCH AND RECOVERY TEAMS
	DEEP SEA VEHICLES/SONAR SYSTEMS
	FIRESCAN IR DETECTION SYSTEM

LiH is used to attenuate the high neutron dose from the 19.5 kg of curium 244. The dose received by persons in the vicinity of an impacted RTPS depends on their distance from the system and the duration of exposure. This chart shows the length of time to receive a whole body dose of 25 rem (maximum reactor accident limit) and 200 rem (observable radiation sickness, with recovery within two weeks) at 1, 3 and 10 meters from radiation surface.

RTPS RADIATION DOSE AFTER LAND IMPACT

DISTANCE FROM SURFACE (METERS)	TIME TO RECEIVE 25 REM (HOURS)	TIME TO RECEIVE 200 REM (HOURS)
1	4.3	34
3	53	427
10	320	2560

The fire shield analysis included both steady-state calculations for bracketing the expected results and transient thermal analysis to determine the time-temperature response of all the major components during and after a 2600°K fire for 10 minutes. Use of the thermal model permitted the fire shield design to benefit from the high inherent thermal capacitance of the RTPS and safety equipment. The major design limit was the auxiliary radiator heat pipe temperature. This limit was set at 1200°K, which represents the 1000-hour rupture stress limit for the heat pipe material.

FIRE SHIELD ANALYSIS METHOD

STEADY STATE:

- ENERGY ABSORPTION
  - SENSIBLE HEAT
  - LATENT HEAT
  - VAPORIZATION HEAT
- TEMPERATURE DROP
  - FIRE ENVIRONMENT
  - INTERNAL HEAT
- HEAT PIPE TEMPERATURE LIMITS

TRANSIENT ANALYSIS:

- GGA TAC-2D THERMAL ANALYZER DIGITAL COMPUTER CODE
- DETAILED MODEL OF ALL SUBSYSTEMS
- CONDUCTIVITY, LATENT HEATS, SPECIFIC HEATS, TEMPERATURE DEPENDENCE
- VARIABLE BOUNDRY CONDITIONS
- LUMPED MODEL USED FOR VERIFICATION

This figure shows fire shield tradeoff curves of LiH and insulation mass with LiH thickness for various values of thermal insulation conductivity. These curves assume that the LiH absorbs all of the fire heat conducted through the insulation by changing from a solid at ambient temperature to a liquid at the boiling point for LiH of 1267°F (960°K). Increasing the LiH thickness diminishes the thickness of insulation required. It can be observed from the lower curves that there is a minimum shield mass for a specific insulation conductivity and LiH thickness. However, to eliminate the requirement of having to remove the shield immediately after the fire, the conductivity of the fire shield should be high enough in the equilibrium case (i.e., radiation of the internal heat to ambient conditions) to limit the operating temperature of the auxiliary heat pipes to approximately 1200°K. To illustrate how the fire shields meet this criteria, the upper curves give the variation in ΔT across the fire shield for different LiH conductivities. This shield design can meet the desired design conditions when the thermal capacitance of the entire system is considered.

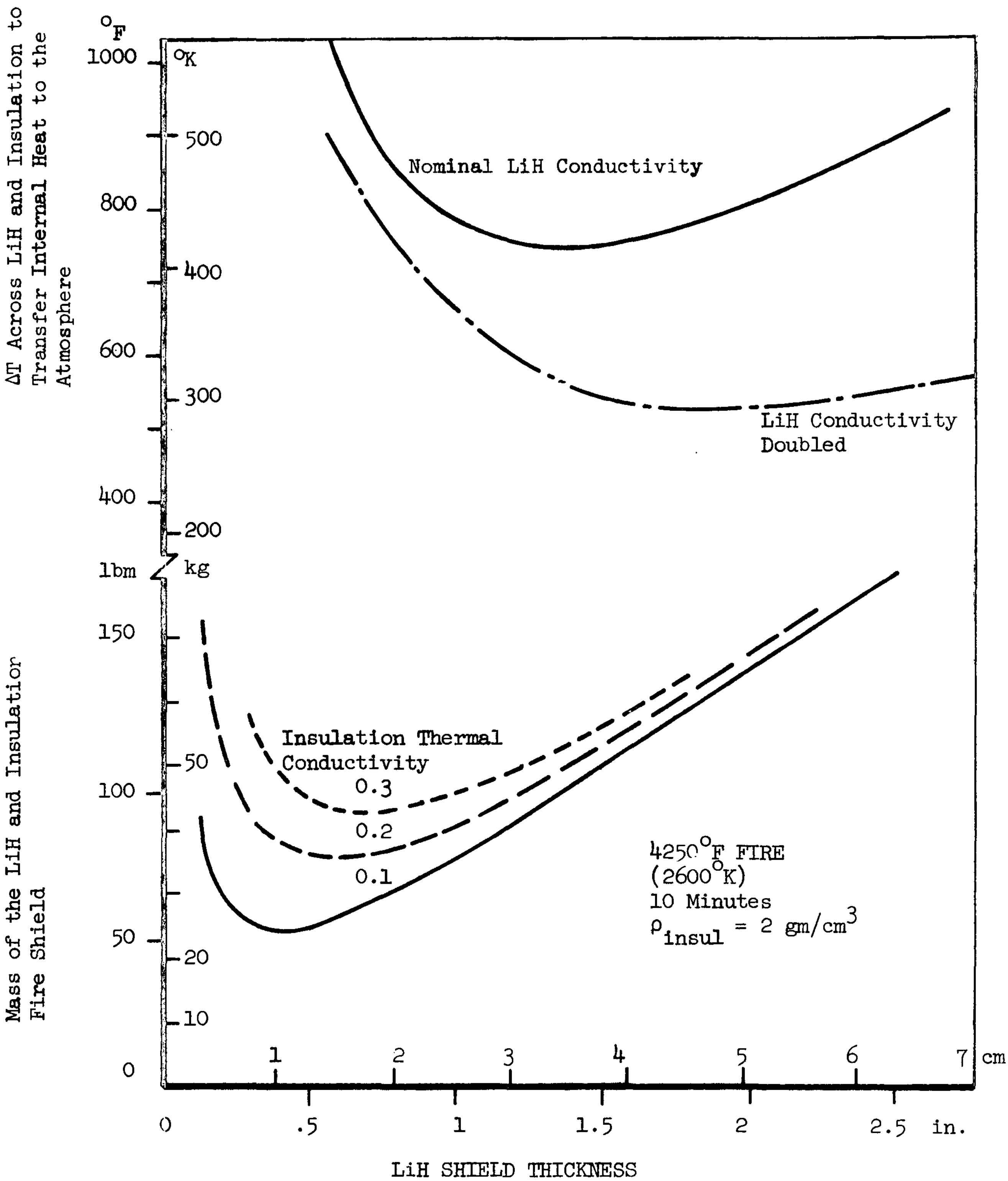

Tradeoff of Fire Shield mass and equilibrium
ΔT with LiH shield thickness

Design of the fire shield was based on the thermal response of the auxiliary radiator heat pipes. The transient thermal response of the heat pipes during and following a launch pad fire was evaluated for various insulation thicknesses, using the detailed thermal model developed for the system. Results of these analyses are summarized in the table. The results for the detailed thermal model show that the heat pipe temperature will be below $1200^{o}K$ for insulation thickness to 0.048-inch, and that the equilibrium temperature at 10^5 seconds (28 hours) for 0.12-inch insulation, is below $1250^{o}K$. Verification of these results was obtained using a simplified lumped thermal model which included a 0.15 cm stainless steel structure around the LiH.

SUMMARY OF TRANSIENT HEAT PIPE TEMPERATURES DURING
A LAUNCH PAD FIRE OF 2600 K FOR 10 MINUTES

Insulation Thickness	Maximum Heat Pipe Temperature in Degree K and (°F)					
	600	1000	3500	10,000	35,000	100,000
	(Time in Seconds)					
0.238" (0.6 cm)	879	914	852	988		
	(1122)	(1186)	(1073)	(1319)		
0.120" (0.3 cm)	935	950	872	966		
	(1223)	(1250)	(1110)	(1278)		
0.120" (0.3 cm) (Revised LiH Properties)*	926	957	896	989	1122	1238
	(1206)	(1262)	(1152)	(1321)	(1559)	(1769)
0.048" (0.12 cm)	1190	1122	936	967	1039	1127
	(1682)	(1560)	(1225)	(1281)	(1411)	(1569)
0.048" (0.12 cm) (N_2 in place of water)	1198	1134	934	985		
	(1697)	(1582)	(1330)	(1313)		

* The LiH/Thermal Conductivity was revised from a constantly decreasing value with temperature, as shown in Table 6.1, to one that leveled off to a value of 2 Btu/hr ft °F above 1760°R.

This figure shows the time temperature history of the LiH shield and heat pipes when exposed to a 2600°K launch pad fire for 10 minutes. The 1.9 cm LiH shield is used for energy storage and is surrounded by 0.31 cm of zirconic felt thermal insulation which attenuates the direct fire heat and protects the LiH containment tanks. The high thermal capacitance of the inner LiH shield (10-cm thick), controls the thermal response following the fire.

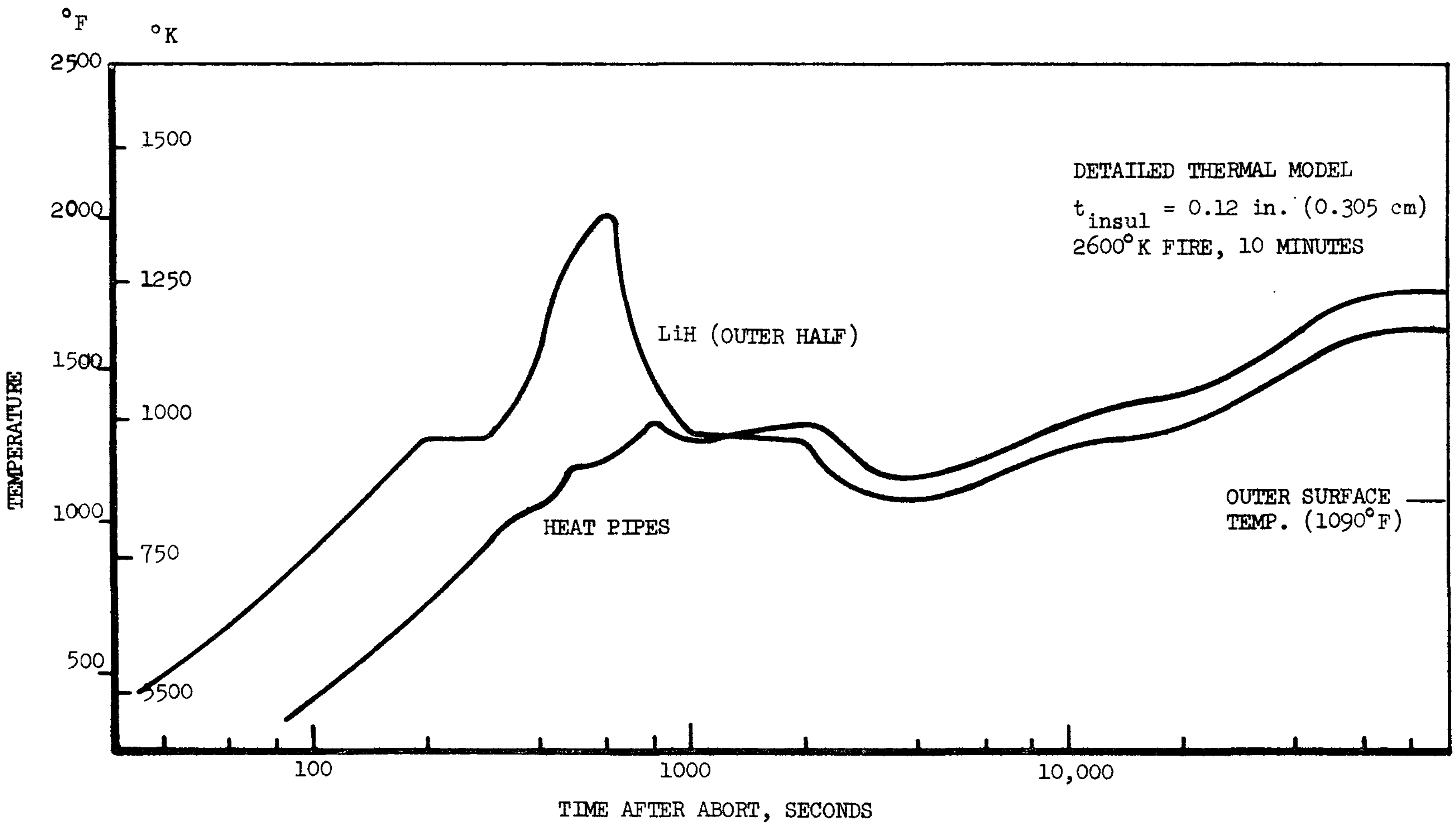
°F
°K
2500
2000
1500
1000
500
1500
1250
1000
750
500
TEMPERATURE
DETAILED THERMAL MODEL
t_{insul} = 0.12 in. (0.305 cm)
2600°K FIRE, 10 MINUTES
LiH (OUTER HALF)
HEAT PIPES
OUTER SURFACE
TEMP. (1090°F)
100
1000
10,000
TIME AFTER ABORT, SECONDS

Design characteristics of the zirconia LiH composite launch pad fire shield are tabulated. This is a completely passive fire shield which does not need to be removed to reject the internally generated isotope heat to the atmosphere. Further optimization of the fire shield would require instrumented thermal tests which would better simulate the insulation thermal response and the effects of interface thermal impedance.

CHARACTERISTICS OF THE REVISED LiH/ZIRCONIA LAUNCH PAD ABORT FIRE SHIELD (2600°K FIRE, 10 MINUTES)

LiH thickness	1.9 cm (0.75 in.)
Stainless steel structure thickness	0.152 cm (0.06 in.)
Zirconia thickness	0.31 cm (0.12 in.)
Shield length	142 cm (361 in.)
LiH density	0.75 gm/cc
Stainless steel density	8.0 gm/cc
Zirconia density	0.9 gm/cc
LiH mass	32.6 kg
Stainless steel mass	28.4 kg
Zirconia mass	6.5 kg
Total shield mass	67.5 kg

This chart shows the masses of heat storage fire shields, assuming that the shield must absorb all of the energy from a 10-minute 2600°K fire by changing phase from a solid to a liquid. Proportionally lower masses would be obtained for shorter fire durations, although the ΔT across the shield is not reduced directly: for example, if LiH were used as a heat storage material for a 60-second fire, its mass would be 90 kg and the resulting equilibrium ΔT to reject the internal heat would be 461°K. Because of the large mass of this type of shield, it was not considered attractive.

HEAT STORAGE FIRE SHIELD DESIGNS

MATERIAL	MASS TO ABSORB $2\,(10)^9$ JOULES (KG)	TEMPERATURE DROP TO REJECT INTERNAL HEAT ($^\circ$ K)
COPPER	10,000	19
LITHIUM HYDRIDE	770	1600
ALUMINUM	5,000	31.2
MAGNESIUM	5,500	71.0
ZINC	18,000	94.1

Four likely abort configurations were studied to determine their reentry aeroballistic characteristics. These are listed in the adjacent table. Three of these are malfunctions occurring near the time of Centaur ignition when suborbital conditions still exist. In the first case, a failure of the Centaur to initiate its chill-down sequence prior to ignition is assumed. In the second case, it is assumed that the chill-down sequence occurs on the Centaur; however, ignition does not occur and the propellants are drained leaving the same assembly as Case 1, but much lighter. The assumption in the third case is that separation of the payload from the Centaur occurs prior to Centaur ignition and the assembly of the payload and RTPS reenters. The final case is the RTPS reentering from earth orbit as a free-body. The stability in the side-on attitude is expressed as $X_{c.p.}/X_{c.g}$ where values >1 are desired. Both Case 1 and 2 will reenter with the Centaur engines forward. Case 3 will tumble and the RTPS as a freebody would be nose first stable. Case 4 was considered as the worst case and was considered for the entire range of reentry possibilities: pre-orbital, orbital, and at escape velocity.

POSSIBLE ABORT CONDITIONS

Configuration	Attitude	Side on X_{cp}/X_{cg}	Ballistic Coefficient	Failure Mode	Comments
1. Fueled Centaur/ payload/RTPS	Centaur engine forward	2.13	415 psf (2028 kg/m^2)	Centaur pre-start sequence not begun	Requires command destruct decision
2. Empty Centaur/ payload/RTPS	Centaur engine forward	1.22	98 (479)	Centaur ignition failure	Requires command destruct decision
3. Payload/RTPS	Tumbling	1.03	21 (103)	Separation failure	Worst sidewall heating
4. RTPS	Nose forward	> 1.20	*	Normal reentry	Worst nose and flare heating

*Ballistic coefficient varies with flare diameter with a range from about 10 to 60 psf. (50-300 kg/m^2)

A range of reentry trajectories were investigated for this design. Reentry trajectories for the reference mission were supplied by the NASA/OART Mission Analysis Division. These were based on a hypersonic drag coefficient of 1.2 and were calculated for a 90^{o} launch azimuth and initial flight path angles from -10^{o} to -90^{o} with an initial velocity of 11 km/sec. Reentry from a low earth orbit was also considered. This figure shows the superorbital reentry profiles. This range of trajectories covers all possible abort modes for the computed reference design ballistic coefficient of 17.5 psf (85.5 kg sm).

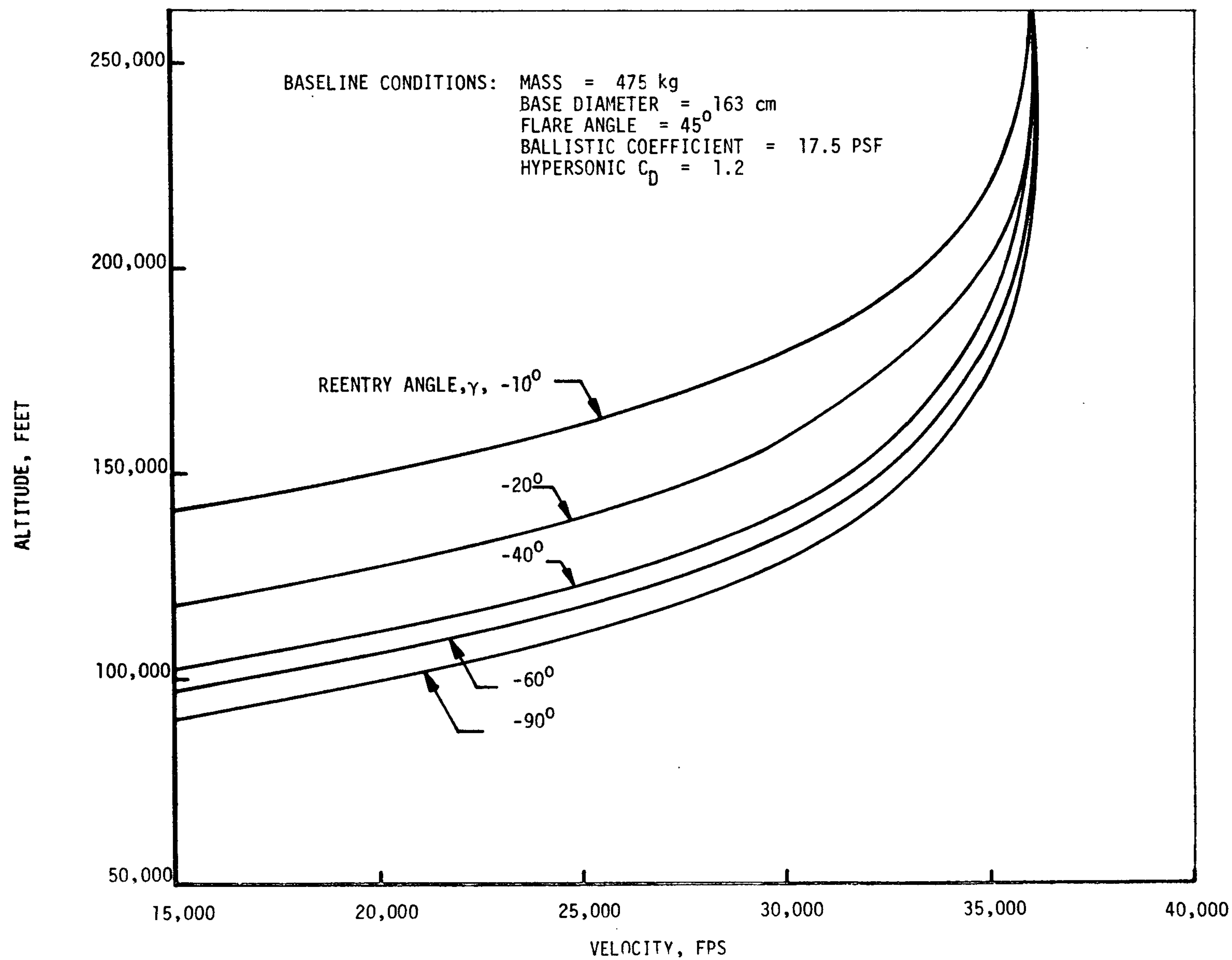

BASELINE CONDITIONS: MASS = 475 kg
BASE DIAMETER = 163 cm
FLARE ANGLE = 45°
BALLISTIC COEFFICIENT = 17.5 PSF
HYPERSONIC C_D = 1.2
REENTRY ANGLE, γ, -10°
-20°
-40°
-60°
-90°
250,000
200,000
150,000
100,000
50,000
ALTITUDE, FEET
15,000
20,000
25,000
30,000
35,000
40,000
VELOCITY, FPS

Transient aerodynamic heating was calculated for each trajectory at four locations on the vehicle: 1) stagnation point; 2) cylinder at 110 cm; 3) cylinder at 180 cm; and 4) flare at 300 cm. Results of these calculations to a cold wall are shown in this figure for two extremes, the short high heat pulse which occurs during a -90° reentry and the longer heat pulse occurring during a -10° reentry.

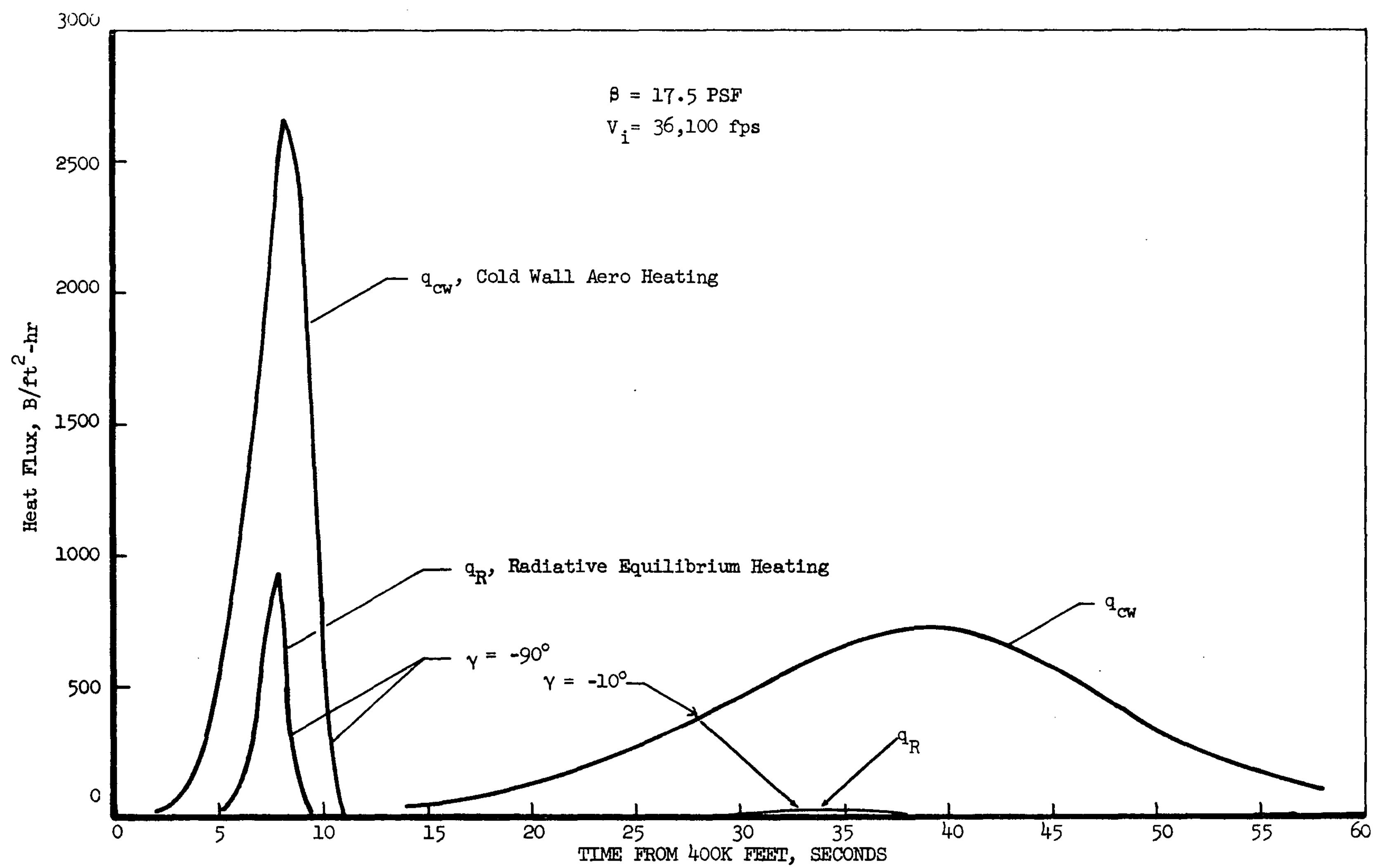

Comparison of Reentry Heating at Stagnation Point

This figure shows the variation in maximum stagnation heating with entry angle at escape velocity. The cold wall and hot wall show the possible extremes in convective heating rates of the surface. The lower curve is based on black body conditions and represents the maximum heating due to radiation.

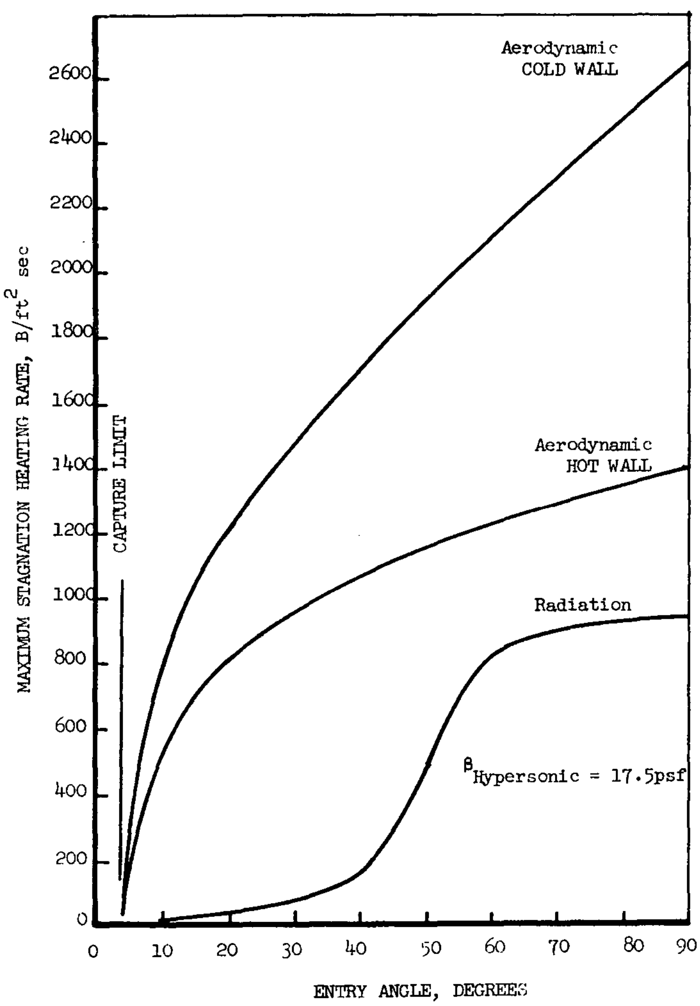

Aerodynamic
COLD WALL
Aerodynamic
HOT WALL
Radiation
β Hypersonic = 17.5psf
CAPTURE LIMIT
MAXIMUM STAGNATION HEATING RATE, B/ft² sec
0
200
400
600
800
1000
1200
1400
1600
1800
2000
2200
2400
2600
0
10
20
30
40
50
60
70
80
90
ENTRY ANGLE, DEGREES

A computer model of the thermal protection system at 4 locations on the vehicle was established using a special reentry heating computer code to calculate transient structural temperatures during reentry from each of the abort trajectories. The model configuration is shown in this figure. Pyrocarb graphite was selected as the ablator, zirconia felt as the insulator, while structural support is provided by stainless steel.

Boundary conditions at the outboard surface were aerodynamic heating, radiative heating (at the stagnation point) and radiation to the environment. In all cases the inboard surfaces were considered to be adiabatic. A heat load of 2.7 KW/ft^2 introduced at the heat pipe zone was also included. Each material layer is divided into segments, as shown, for an accurate conduction analysis. Temperatures are calculated for each vehicle location based on an instantaneous, heat balance at the outboard surface, while accounting for the radiative heat rejection at the surface and the inboard conduction to underlying layers. The thermophysical properties of specific heat and thermal conductivity were allowed to vary with local segment temperature.

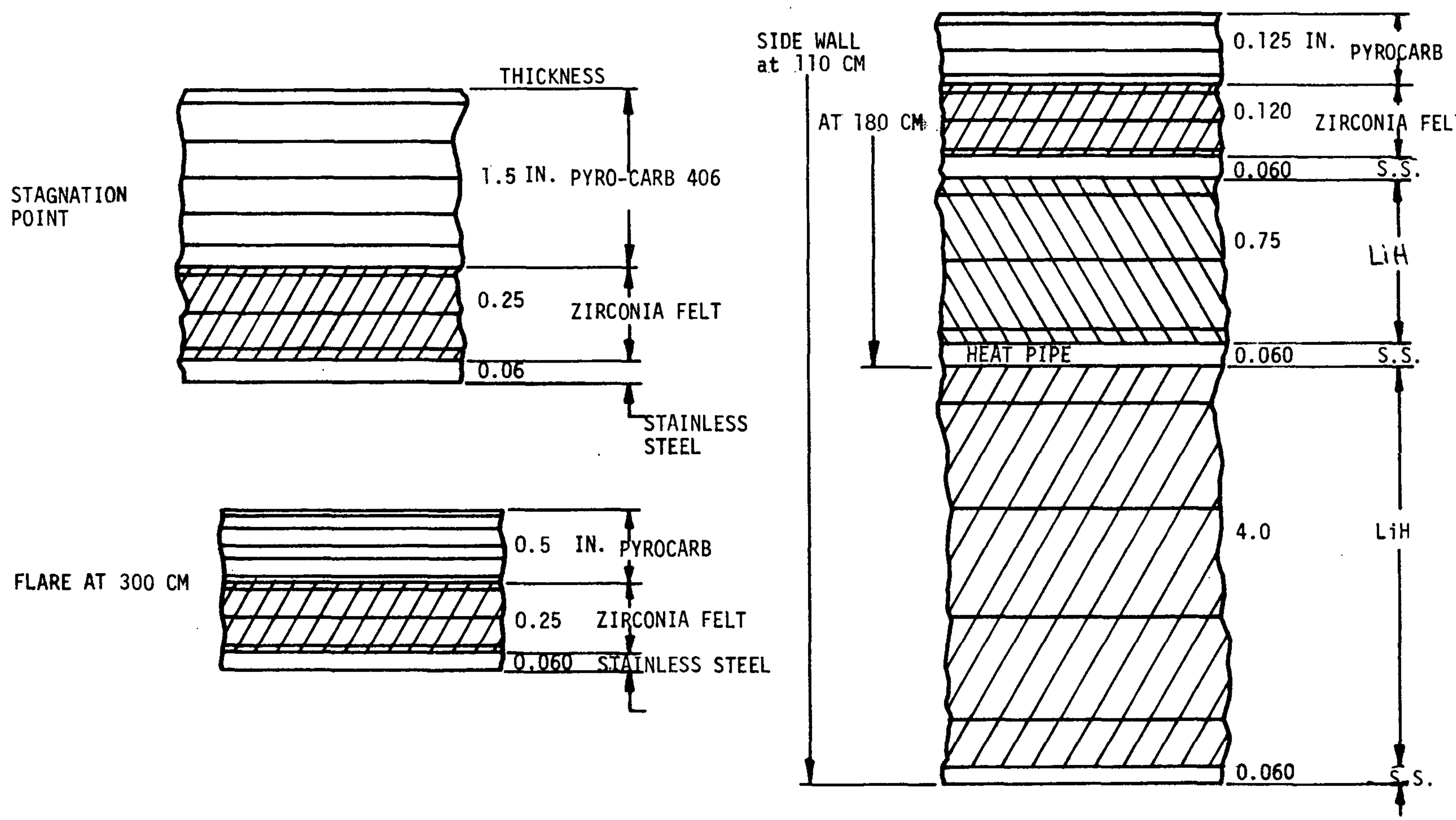

THICKNESS
STAGNATION POINT
1.5 IN. PYRO-CARB 406
0.25 ZIRCONIA FELT
0.06
STAINLESS STEEL
FLARE AT 300 CM
0.5 IN. PYROCARB
0.25 ZIRCONIA FELT
0.060 STAINLESS STEEL
SIDE WALL at 110 CM
AT 180 CM
0.125 IN. PYROCARB
0.120 ZIRCONIA FELT
0.060 S.S.
0.75 LiH
HEAT PIPE
0.060 S.S.
4.0 LiH
0.060 S.S.

Maximum reentry temperatures calculated for each vehicle location and for each trajectory are given in this table. The most severe heating of the stainless steel structure generally occurs during orbital decay reentry for which the long heat pulse allows significant inboard heat conduction. The highest external temperatures occur during the steep reentry. Tumbling heating corresponding to Case 3 for a separation failure case was not calculated but should closely correspond to side wall temperatures for the -90° reentry case.

MAXIMUM REENTRY TEMPERATURES

Ballistic Coefficient, $\beta = 17.5$ psf
($85.5\ kg/m^2$)

Location	Reentry Angle,	$\gamma = -90^\circ$	-60°	-40°	-20°	-10°	0°
		(Temperatures in °K)					
Stag. Pt:	Outer Pyro-Carb	4070°K	3880	3428	3246	3010	1981
	Inner Pyro-Carb	1507	1473	1566	1893	2324	1945
	Structure	713	703	727	811	925	1252
Sidewall @110 cm :	Outer Pyro-Carb	1050	1010	1003	963	913	720
	Outer Structure	886	886	887	891	896	926
	Heat Pipe	943	943	944	947	981	967
	Inner Structure	883	883	883	883	883	885
Sidewall @ 180 cm:	Outer Pyro-Carb	1042	1001	1010	987	946	724
	Structure	886	886	888	893	900	933
	Heat Pipe	968	970	972	976	981	1015
Flare @ 300 cm	Outer Pyro-Carb	4383	4028	3871	3405	3013	1156
	Inner Pyro-Carb	2651	2469	2658	2813	2812	1152
	Structure	681	658	680	719	799	662

This figure shows transient reentry temperatures for the two extreme entry angle cases. The results show that the reentry shield provides an adequate design margin for the underlying structure of stainless steel, which can operate above 1200°K for short durations.

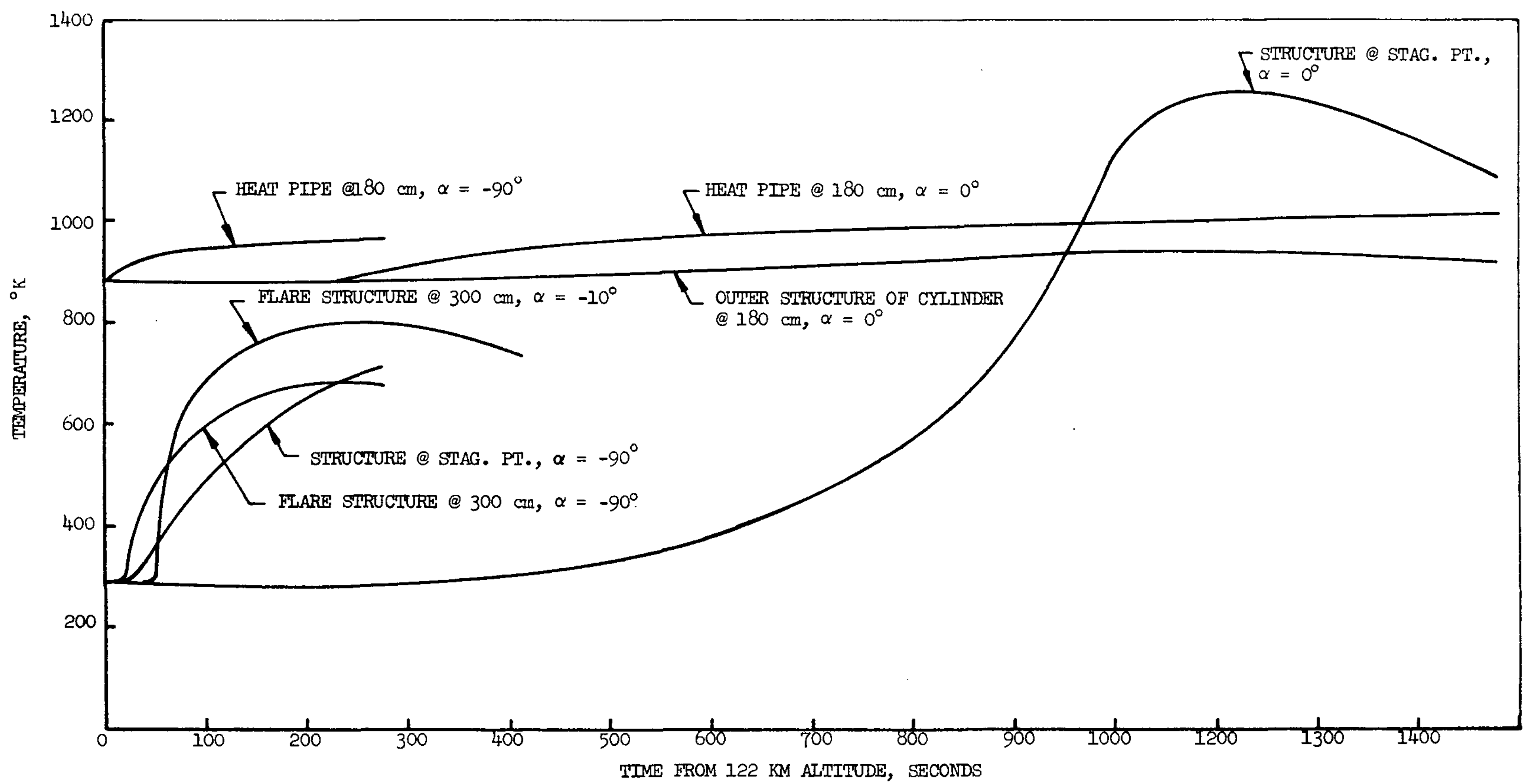

STRUCTURE @ STAG. PT., α = 0°
HEAT PIPE @180 cm, α = -90°
HEAT PIPE @ 180 cm, α = 0°
FLARE STRUCTURE @ 300 cm, α = -10°
OUTER STRUCTURE OF CYLINDER @ 180 cm, α = 0°
STRUCTURE @ STAG. PT., α = -90°
FLARE STRUCTURE @ 300 cm, α = -90°
TEMPERATURE, °K
1400
1200
1000
800
600
400
200
0
100
200
300
400
500
600
700
800
900
1000
1200
1300
1400
TIME FROM 122 KM ALTITUDE, SECONDS

Transient mass loss rates are shown for the extremes of reentry at superorbital velocities. Although a very high mass loss rate is experienced during - 90^{o} reentry due to sublimation, a greater mass loss occurs during -10^{o} reentry as a result of the substantially longer heat pulse. Corresponding dimensional change of the Pyro-Carb 406 is 0.82 inch and 1.43 inch, respectively.

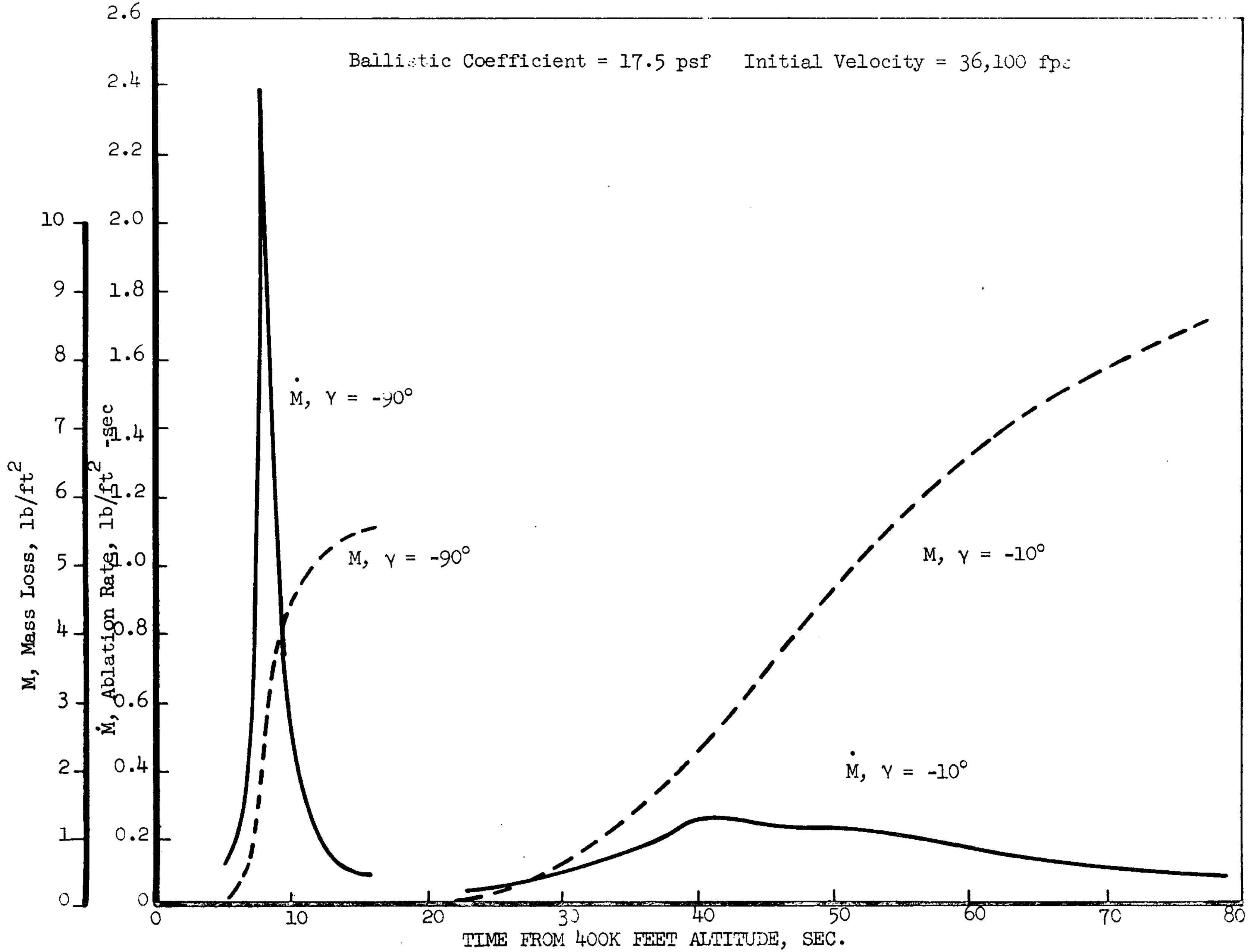

Stagnation Point Ablation

The influence of variations in the diameter of the 45° half-angle flare on the RTPS aeroballistics are shown. Volume within the payload envelope allows for a substantial increase in the flare diameter above the 122 cm diameter baseline design. Benefits of a larger flare are to reduce the ballistic coefficient of the configuration. These calculations assumed the unit weight of the flare is 8 kg/m^2. The design point diameter of 8 feet 2.44 meters shown in the figure was selected since it results in ballistic coefficients below the knee of the curve and does not cause excessive weight.

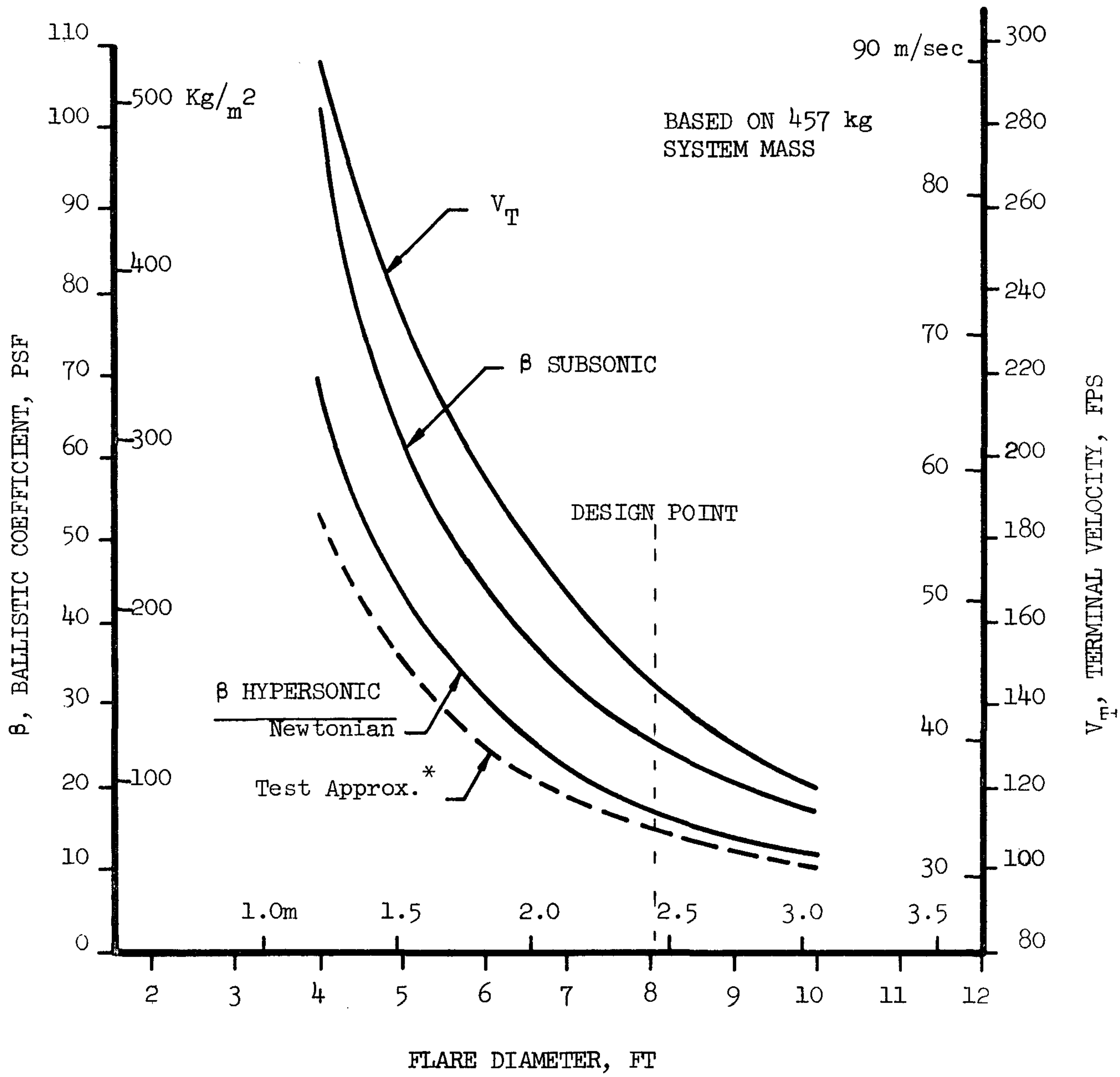

*Extrapolated from test data of similar shape at 4 ft flare (Ref. 15)

Variation of aeroballistic parameters with flare size

Parachutes were used during the initial studies for the RTPS for drag augmentation to limit the earth impact terminal velcoity to 26 m/sec. Without parachutes the velocity would be 89 m/sec (292 fps) for the original 122-cm diameter flare. However, a significant reduction in terminal velocity can be realized by increasing the flare diameter. The impact velocity is approximately proportional to the reciprocal of the flare diameter, while the mass of the flare varies as the square of the diameter. The influence of flare diameter and angle on mass of the honeycomb and flare is shown on this chart. A 45° angle was selected based on aerodynamic heating considerations.

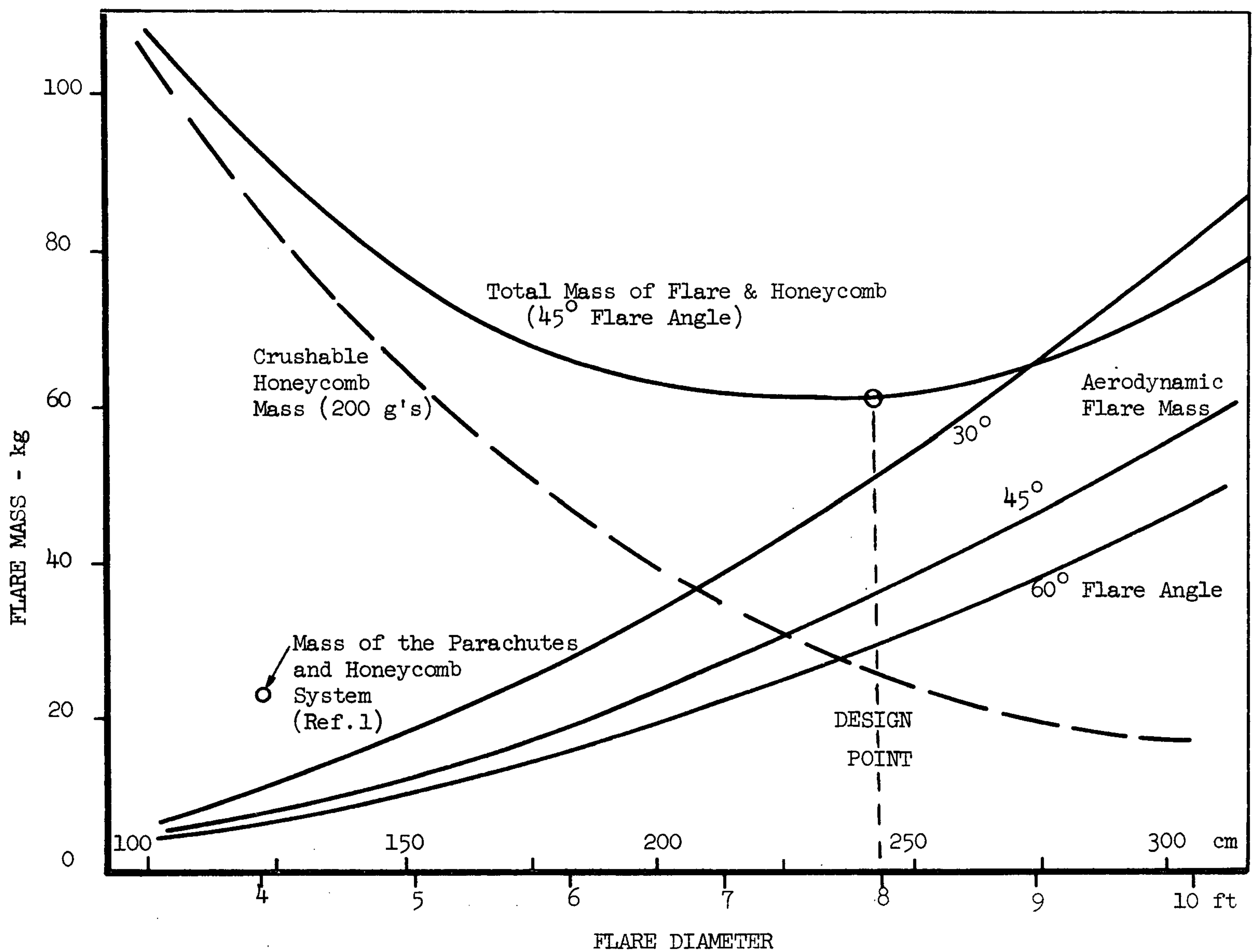

Tradeoff of RTPS Aerodynamic flare mass and honeycomb energy absorber mass with flare diameter

Protection of the fuel during land impact is provided by an aluminum honeycomb energy absorption column and an aerodynamic flare retardation device. These systems are designed to limit the deceleration rate to 200 gs to assure integrity of the safety system structure. The honeycomb energy absorber designs considers effects of a 20 mph wind and the honeycomb crushing efficiency. Also considered was earth burial and rotational moments during impact.

IMPACT PROTECTION SYSTEM

DESIGN TERMINAL VELOCITY	45 M/SEC (147 FPS)
DESIGN IMPACT DECELERATION	200 G's
HONEYCOMB THICKNESS	0.73 M
KINETIC ENERGY ABSORBED	$4.8(10)^5$ J
HONEYCOMB MASS	25.1 KG
AERODYNAMIC FLARE MASS	35.7 KG
IMPACT PROTECTION MASS	60.8 KG

The influence of added LiH biological shielding on the sea level terminal velocity is shown for three different flare designs. These curves are based on scaling relations between increased vehicle diameter and sub-component masses as well as increased LiH mass. A 200 kg increase in system mass will lower the dose rate by a factor of 3 and increase the diameter by 20 cm.

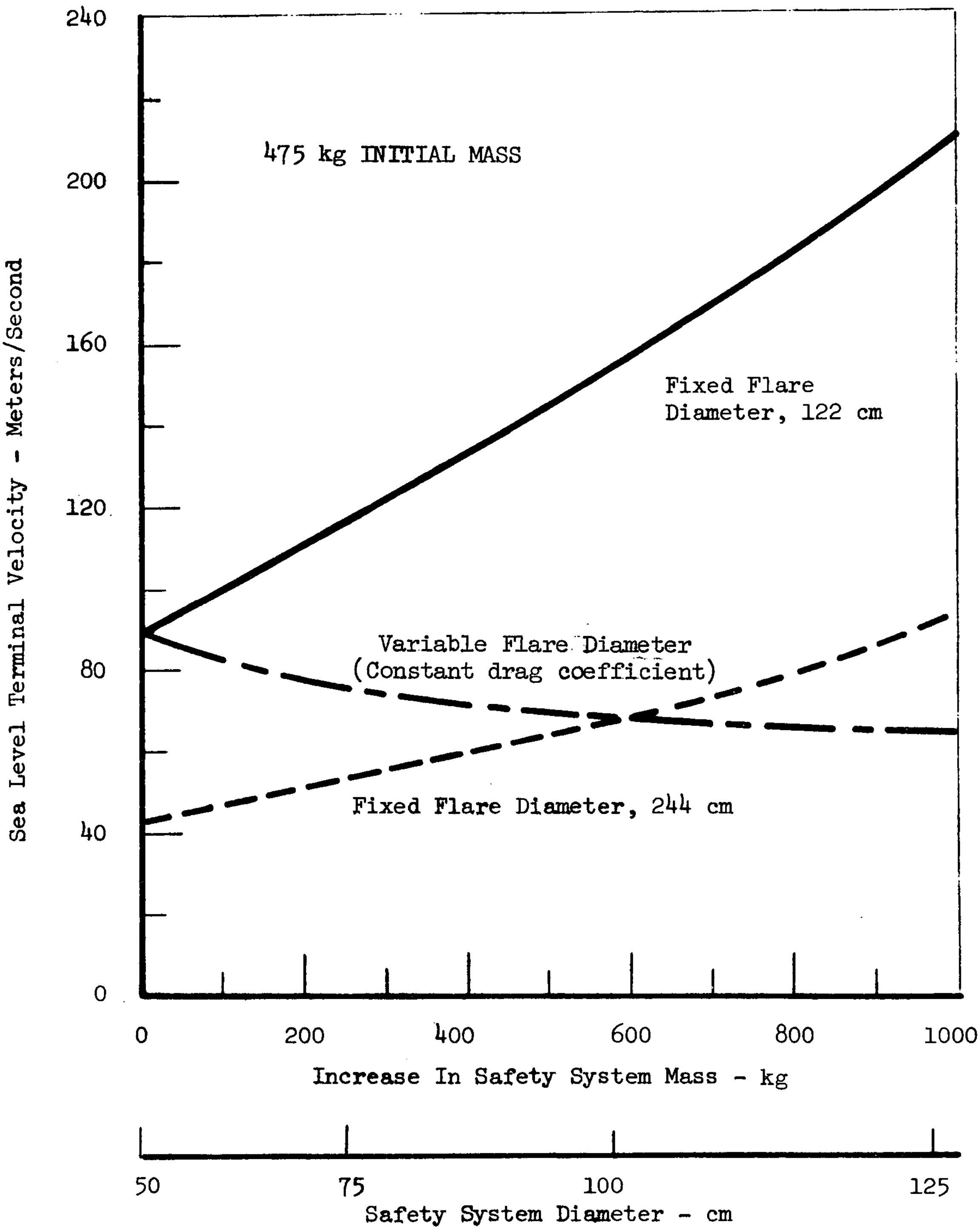

Sea level terminal velocity changes with increases in safety system mass and diameter

Tradeoffs in RTPS diameter and auxiliary radiator surface temperature are shown. The results indicate that most of the heat is transferred by radiation, and that partial burial will result in up to $160^{\circ}K$ increase in radiator temperature. However, this is conservative in that it neglects conduction to the ground. The limiting temperature of the auxiliary radiator is based on the strength of the stainless-steel clad potassium heat pipes, which can operate for short times at $\sim 1400^{\circ}K$ and for longer times at $1200^{\circ}K$.

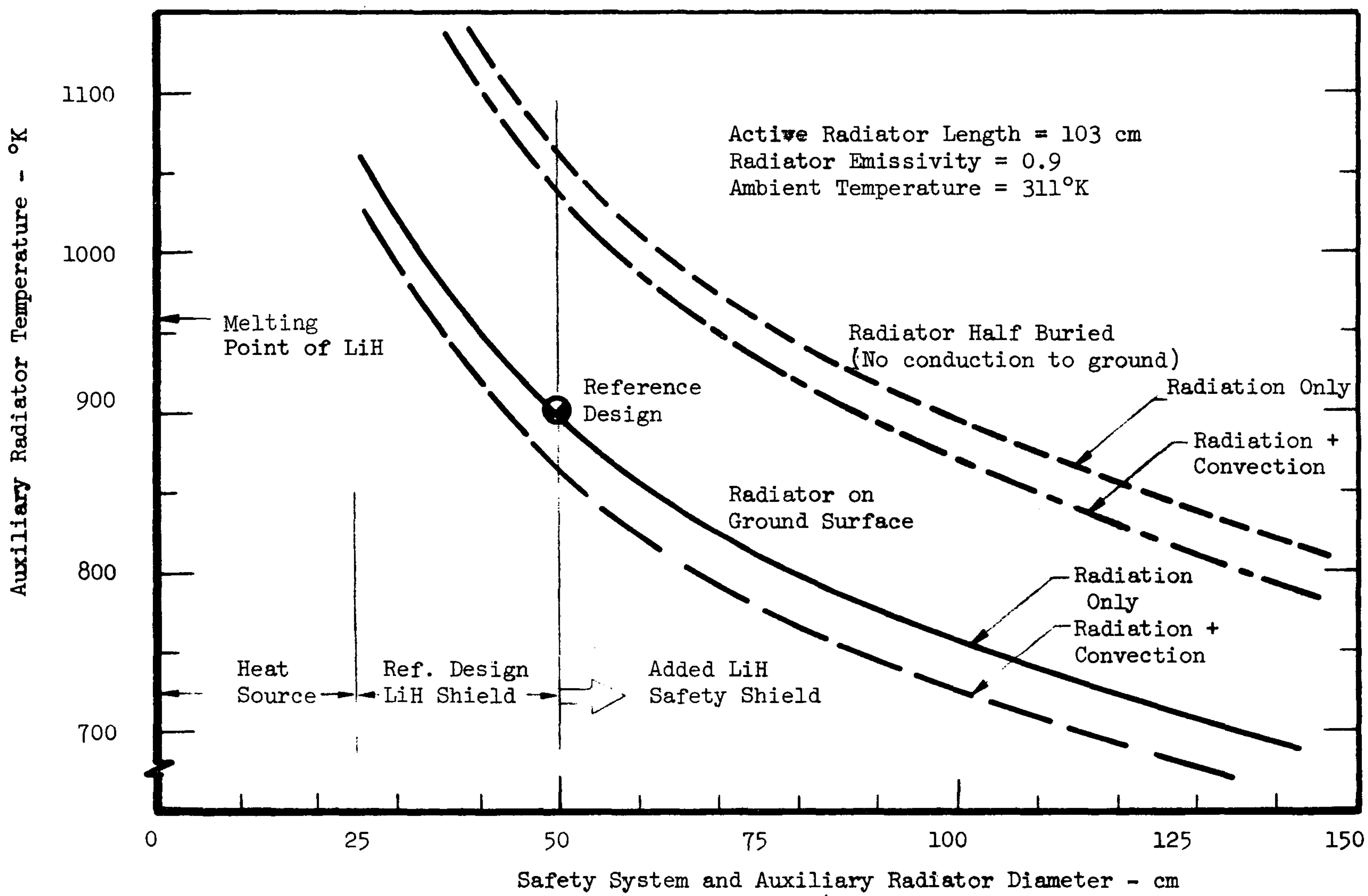

Post Impact Temperature of Auxiliary Radiator Versus Radiator Diameter

This plot shows the tradeoffs in neutron dose rates from the Cm-244 fuel with added thickness and associated mass of LiH shielding. The curves also show the necessary exclusion distance to lower the dose and resulting radiation hazard. Distances shown correspond approximately to: (1) surface conditions, (2) the closest reasonable distance for short-term exposure, and (3) a representative distance for the immediate surrounding area which could be used as an estimate for longer term exposure.

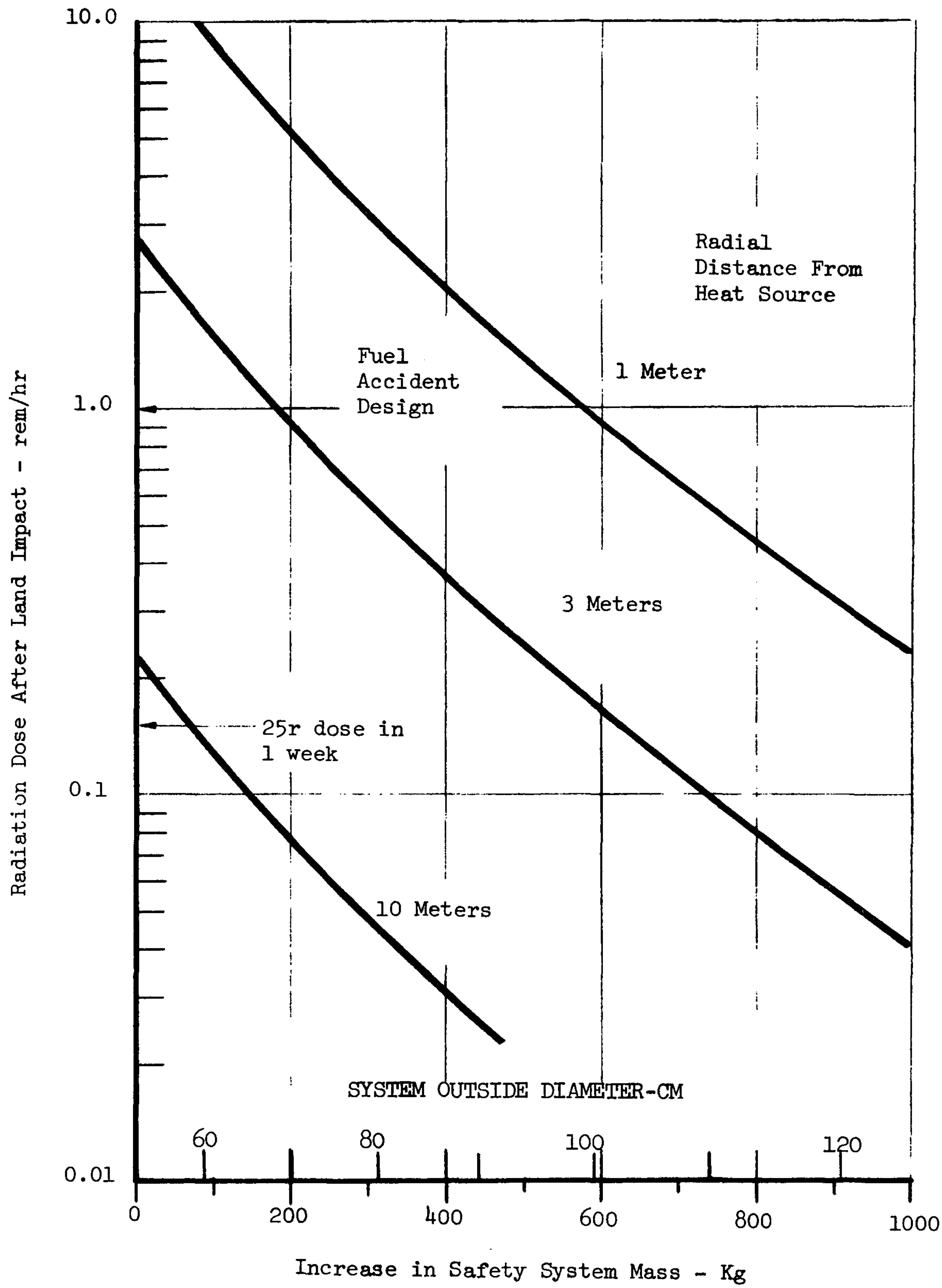

Radial dose rates from heat source after impact
versus increase in mass

An estimate was made of the procurement costs for a complete flight system. Unit costs assumed and itemized total costs for individual components are shown. The major cost change in this phase of the study is a reduction in isotope cost resulting from the reduced mission time and shorter period for radioisotope decay.

FLIGHT SYSTEM COSTS

	Unit Cost	Item Cost (10^3 $)
$Curium^{244}$ Fuel	$ 100/thermal watt	4,420
Encapsulation costs	$ 15,000/capsule	2,040
Emitter heat pipes	$ 5,000	345
Thermionic converters	$ 5,000	345
Radiator heat pipes	$ 2,000	138
Power conditioning	$ 2,000/module	16
Beryllium shield	$ 700/lb	38
Heat source case & insulation		20
Safety System		
Auxiliary heat pipes	$ 750	300
Fire shield		30
LiH shielding		50
Reentry heat shield		60
Structure		40
Assembly operations		200
Launch support equipment		100
Auxiliary prelaunch shielding		30
	TOTAL	8,172